

In the format provided by the authors and unedited.

De novo-designed translation-repressing riboregulators for multi-input cellular logic

Jongmin Kim^{1,2,13}, Yu Zhou^{3,4,13}, Paul D. Carlson^{5,6}, Mario Teichmann⁷, Soma Chaudhary^{3,4}, Friedrich C. Simmel^{1,7,8}, Pamela A. Silver^{1,9}, James J. Collins^{1,10,11}, Julius B. Lucks^{1,6,12}, Peng Yin^{1,9*} and Alexander A. Green^{1,3,4*}

¹Wyss Institute for Biologically Inspired Engineering, Harvard University, Boston, MA, USA. ²Integrative Biosciences and Biotechnology, Pohang University of Science and Technology, Pohang, Gyeongbuk, Republic of Korea. ³Biodesign Center for Molecular Design and Biomimetics, The Biodesign Institute, Arizona State University, Tempe, AZ, USA. ⁴School of Molecular Sciences, Arizona State University, Tempe, AZ, USA. ⁵Robert F. Smith School of Chemical and Biomolecular Engineering, Cornell University, Ithaca, NY, USA. ⁶Center for Synthetic Biology, Northwestern University, Evanston, IL, USA. ⁷Physics Department E14 and ZNN/WSI, Technische Universität München, Garching, Germany. ⁸Nanosystems Initiative Munich, Munich, Germany. ⁹Department of Systems Biology, Harvard Medical School, Boston, MA, USA. ¹⁰Institute for Medical Engineering and Science, Department of Biological Engineering, and Synthetic Biology Center, Massachusetts Institute of Technology, Cambridge, MA, USA. ¹¹Broad Institute of MIT and Harvard, Cambridge, MA, USA. ¹²Department of Chemical and Biological Engineering, Northwestern University, Evanston, IL, USA. ¹³These authors contributed equally: Jongmin Kim, Yu Zhou. *e-mail: py@hms.harvard.edu; alexgreen@asu.edu

Supplementary Information for “De novo-designed translation-repressing riboregulators for multi-input cellular logic”

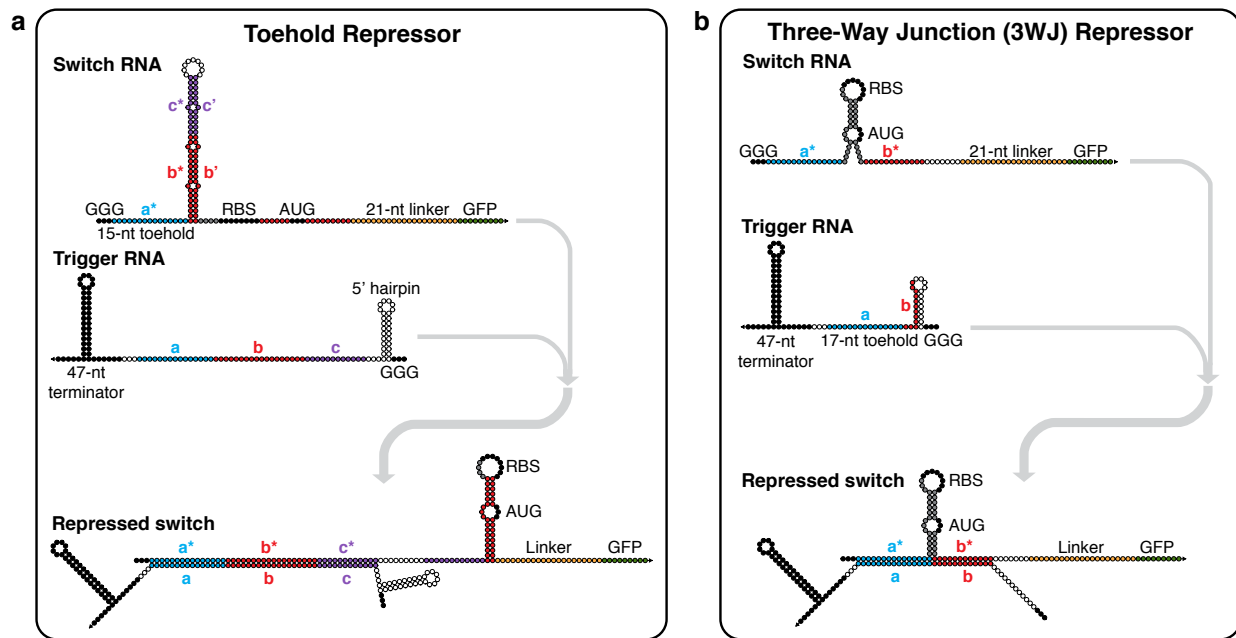
Jongmin Kim^{1,2†}, Yu Zhou^{3,4†}, Paul D. Carlson^{5,6}, Mario Teichmann⁷, Soma Chaudhary^{3,4}, Friedrich C. Simmel^{7,8}, Pamela A. Silver^{1,9}, James J. Collins^{1,10,11}, Julius B. Lucks^{6,12}, Peng Yin^{1,9}, Alexander A. Green^{3,4*}*

¹Wyss Institute for Biologically Inspired Engineering, Harvard University, Boston, Massachusetts 02115, USA. ²Integrative Biosciences and Biotechnology, Pohang University of Science and Technology, Pohang, Gyeongbuk 37673, Republic of Korea. ³Biodesign Center for Molecular Design and Biomimetics, The Biodesign Institute, Arizona State University, Tempe, Arizona 85287, USA. ⁴School of Molecular Sciences, Arizona State University, Tempe, Arizona 85287, USA. ⁵Robert F. Smith School of Chemical and Biomolecular Engineering, Cornell University, Ithaca, New York 14853, USA. ⁶Center for Synthetic Biology, Northwestern University, Evanston, Illinois 60208, USA. ⁷Physics Department E14 and ZNN/WSI, Technische Universität München, Garching 85748, Germany. ⁸Nanosystems Initiative Munich, Munich 80799, Germany. ⁹Department of Systems Biology, Harvard Medical School, Boston, Massachusetts 02115, USA. ¹⁰Institute for Medical Engineering and Science, Department of Biological Engineering, and Synthetic Biology Center, Massachusetts Institute of Technology, Cambridge, Massachusetts 02139, USA. ¹¹Broad Institute of MIT and Harvard, Cambridge, Massachusetts 02142, USA. ¹²Department of Chemical and Biological Engineering, Northwestern University, Evanston, IL, 60208, USA

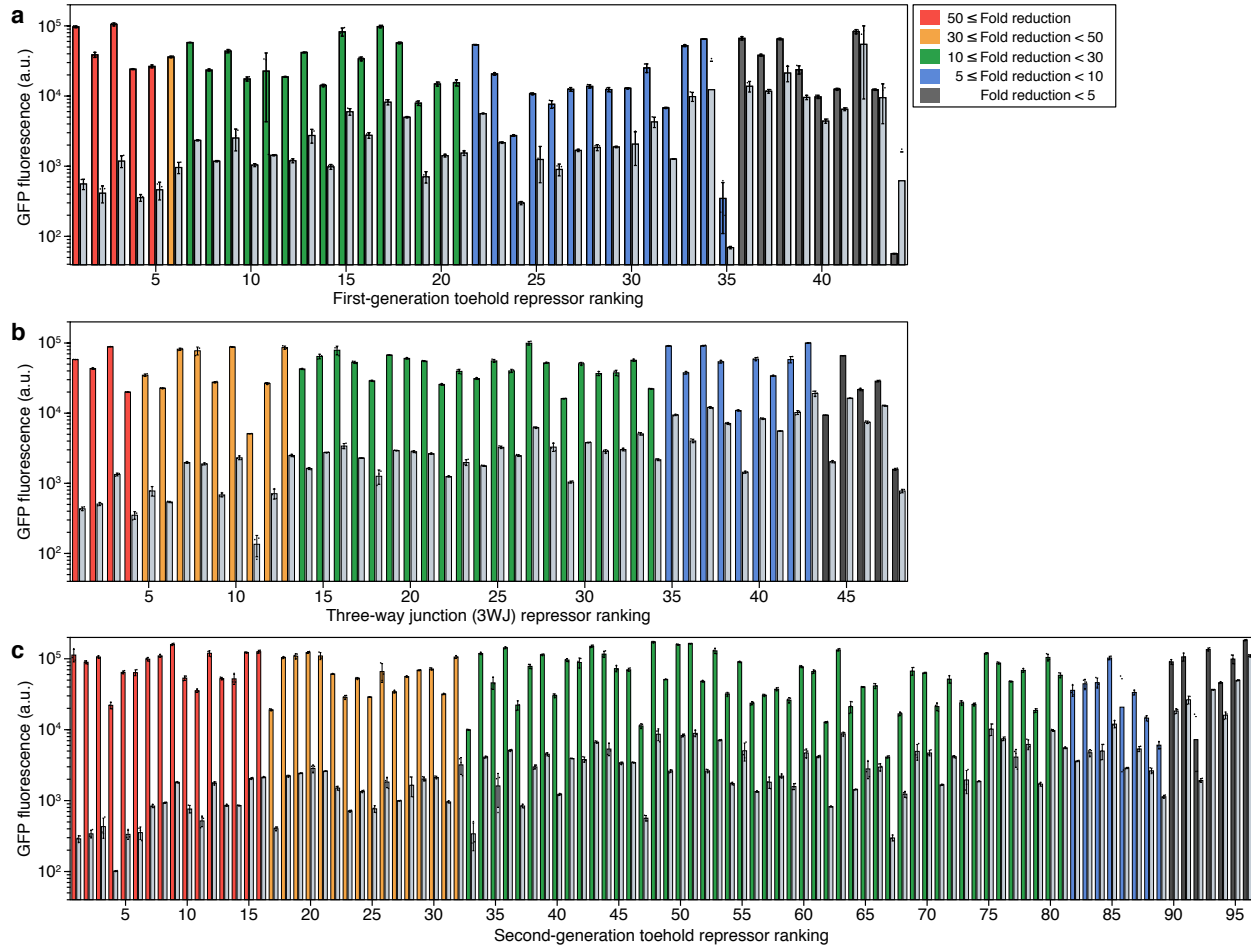
[†] These authors contributed equally to this work

* Correspondence to: alexgreen@asu.edu, py@hms.harvard.edu

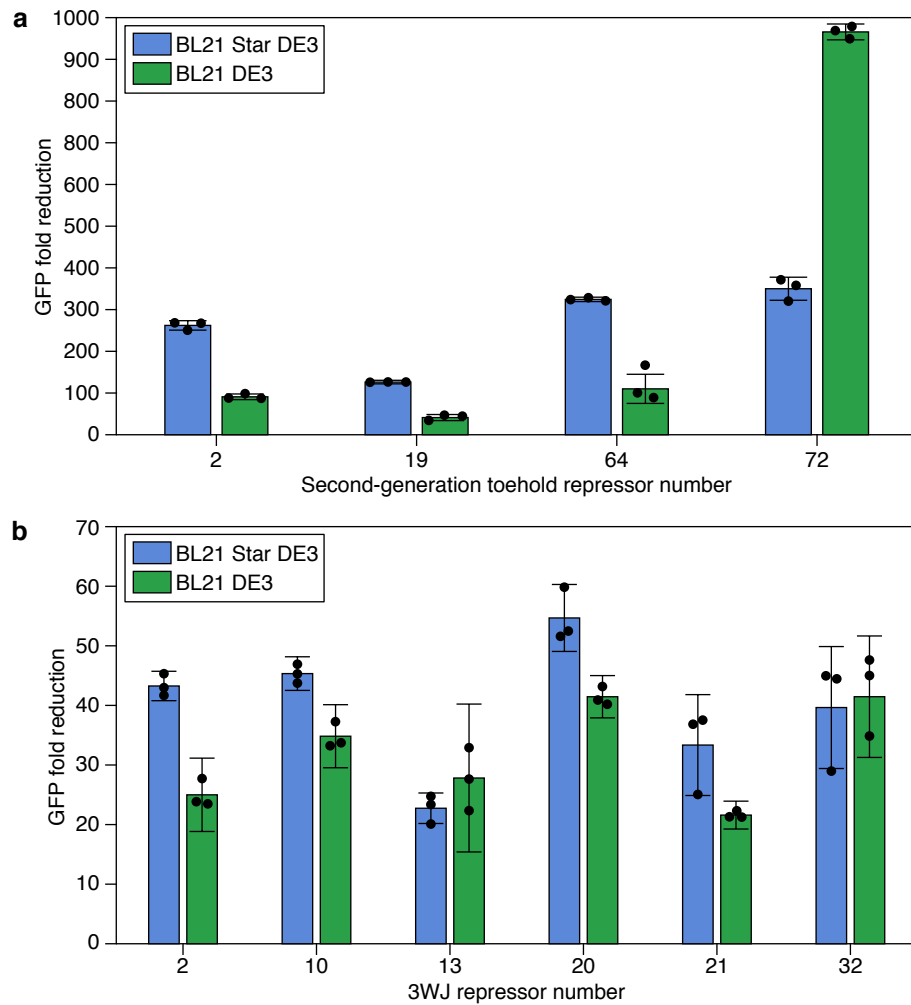
Supplementary Figures



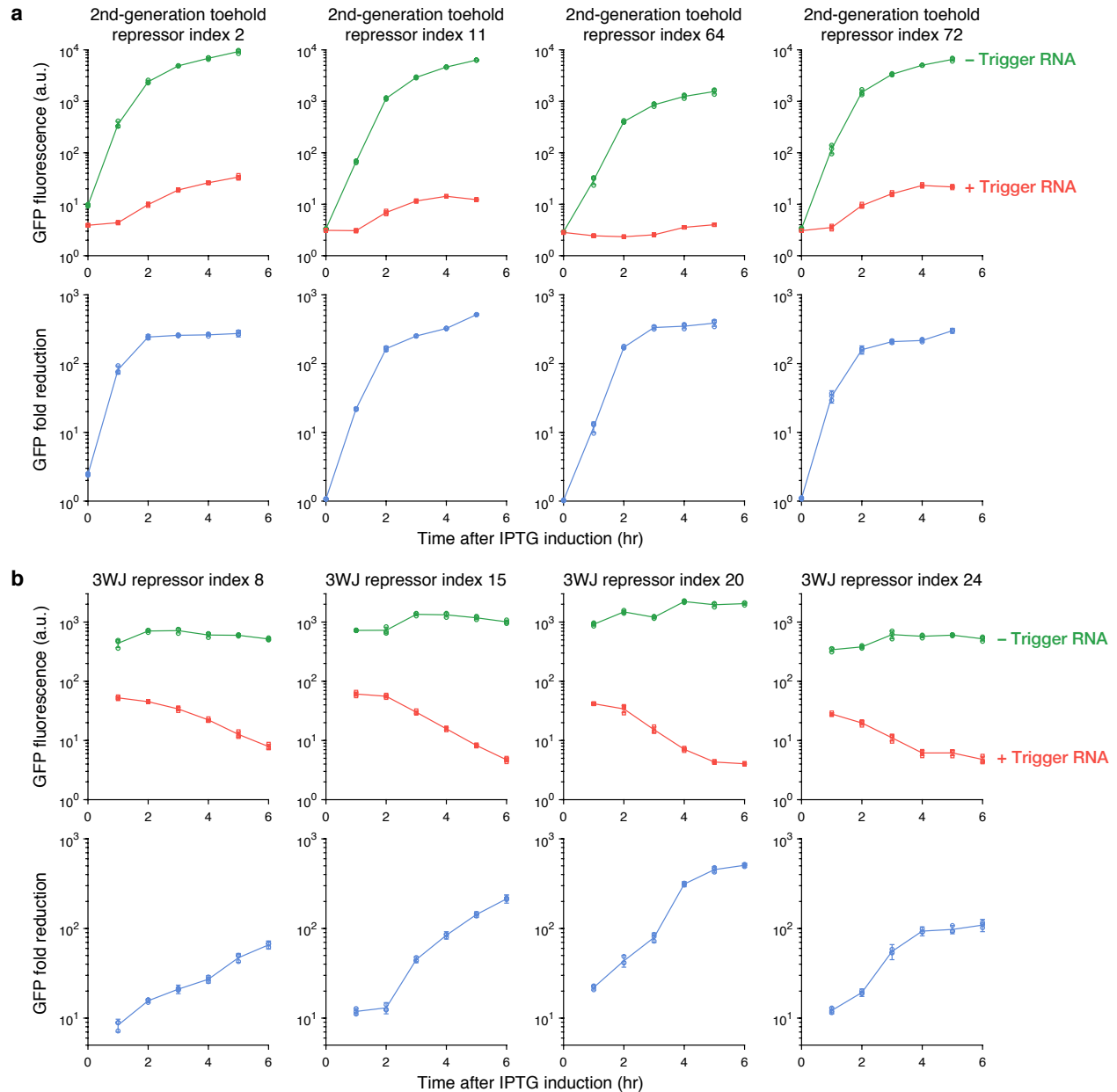
Supplementary Figure 1 | Nucleotide-level schematics of toehold repressors and three-way junction (3WJ) repressors. **a**, Toehold repressors employ a switch RNA with a 15-nt toehold and a 30-nt stem to interact with a trigger RNA with a 45-nt single-stranded region. Binding of the trigger causes formation of a translation-repressing hairpin structure. **b**, Three-way junction repressors employ a conserved hairpin structure in the switch RNA that places binding domains **a*** and **b*** in close proximity while still enabling effective translation. Binding of the trigger RNA through a toehold-mediated interaction forms a 3WJ structure that represses translation. Black bases designate sequences that are biologically conserved (e.g. terminators, RBS, start codons). White bases indicate sequences determined by NUPACK based on the specified secondary structure. Gray bases indicate sequences derived from previous riboregulators.



Supplementary Figure 2 | GFP fluorescence of the toehold and 3WJ repressor libraries. **a-c**, GFP fluorescence levels measured via flow cytometry for the switch RNA expressed with a non-cognate trigger with high secondary structure (colored bars, ON state) and with the cognate trigger (gray bars, OFF state) for the first-generation toehold repressors (a), 3WJ repressors (b), and second-generation toehold repressors (c). Repressors were measured 3 hr after induction. GFP fluorescence and error bars are from the arithmetic mean and the standard deviation (SD), respectively, of n=3 biologically independent samples. Individual points show the fluorescence measured from each biologically independent sample.

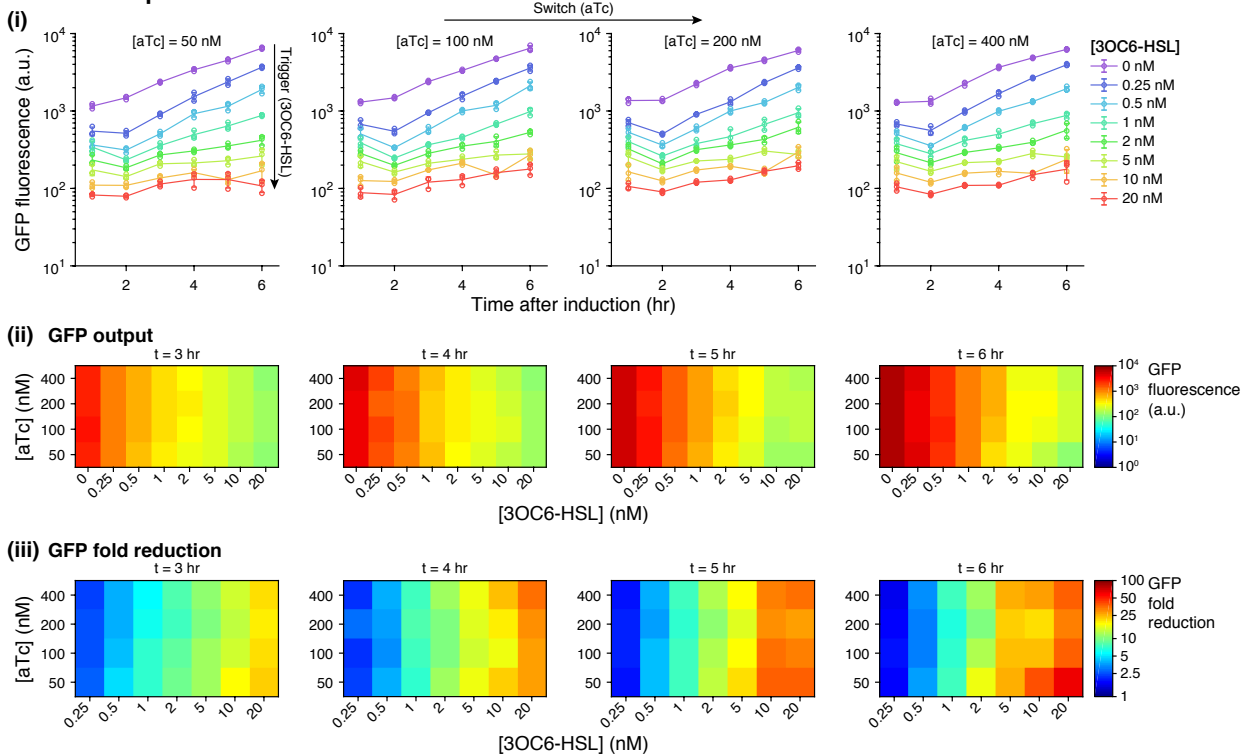


Supplementary Figure 3 | GFP fold reduction measured from synthetic repressors in different *E. coli* strains. **a**, Comparison of GFP fold reduction for second-generation toehold repressors in *E. coli* BL21 Star DE3, which is RNase deficient, with *E. coli* BL21 DE3, which has wild-type RNase levels. The toehold repressors exhibit device dependent variations with strain but provide >40-fold reduction levels. Cells were measured via flow cytometry after 4 hours of induction with 0.1 mM IPTG. **b**, Comparison of GFP fold reduction in the same two strains for 3WJ repressors. The devices show comparable fold reductions in both strains. Cells were measured via flow cytometry after 5 hours of induction with 0.1 mM IPTG. Fold reduction is the ratio of the arithmetic mean of the GFP fluorescence level for the ON and OFF translation states and the relative errors for the ON and OFF states are from the SD of n=3 biologically independent samples. Relative errors for GFP fold reduction were obtained by adding the relative errors of the repressor ON- and OFF-state fluorescence measurements in quadrature. Individual points show the fold reduction from n=3 pairs of biologically independent samples.

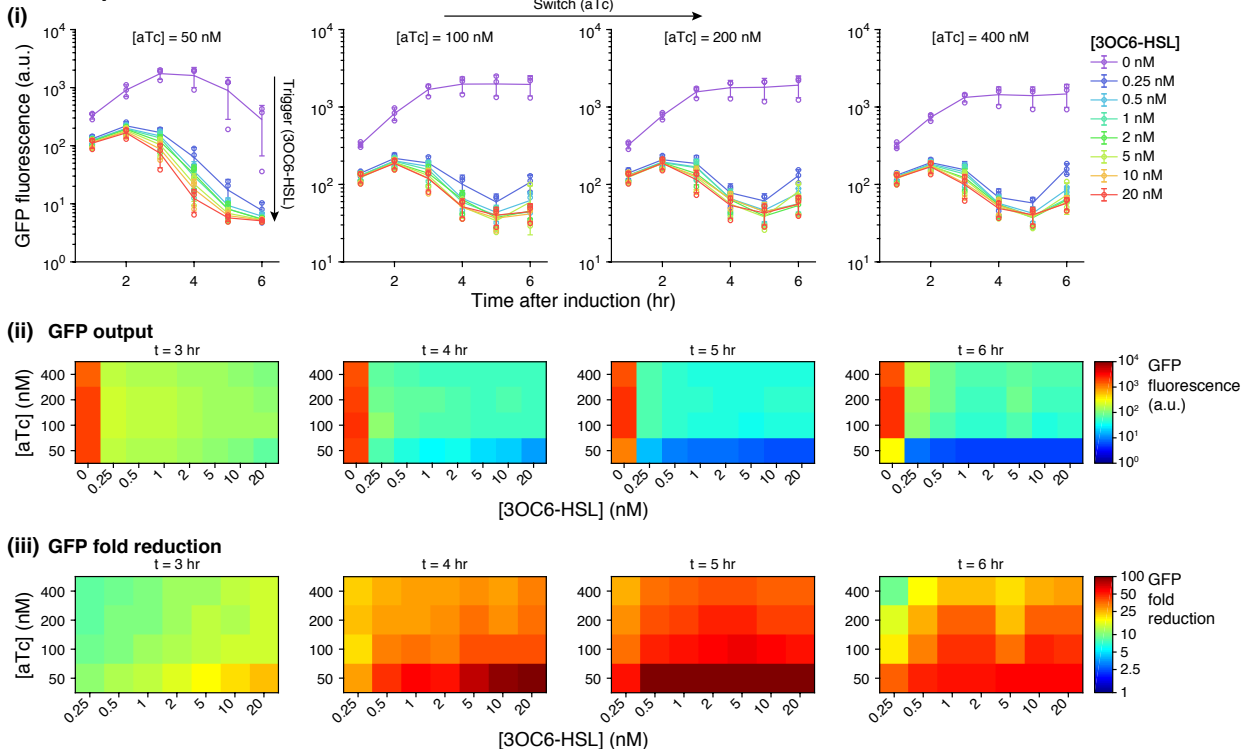


Supplementary Figure 4 | Time-course measurements of toehold and 3WJ repressors. **a**, Toehold repressors display increasing GFP expression as induction time increases. Strong fold reductions are observed within an hour of induction and increase over time. **b**, 3WJ repressors display a relatively weaker increase in GFP expression over time in the absence of the trigger compared to the toehold repressors, while GFP levels in the presence of the trigger decrease over time. Fold reductions reach ~10-fold within an hour of induction and increase over time. GFP fluorescence values and their errors are the arithmetic mean and SD, respectively, of $n=3$ biologically independent samples. Fold reduction is the ratio of the GFP fluorescence values for the ON and OFF translation states. Relative errors for GFP fold reduction were obtained by adding the relative errors of the repressor ON- and OFF-state fluorescence measurements in quadrature. Individual points show fluorescence from $n=3$ biologically independent samples or the fold reduction from $n=3$ pairs of biologically independent samples.

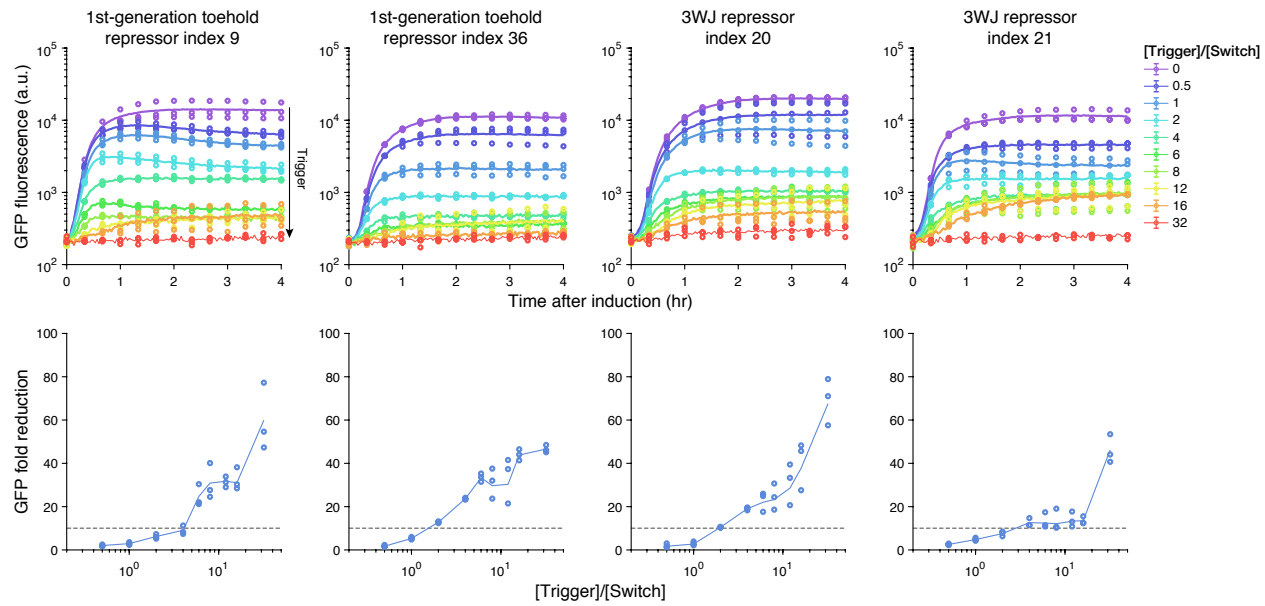
a Toehold repressor



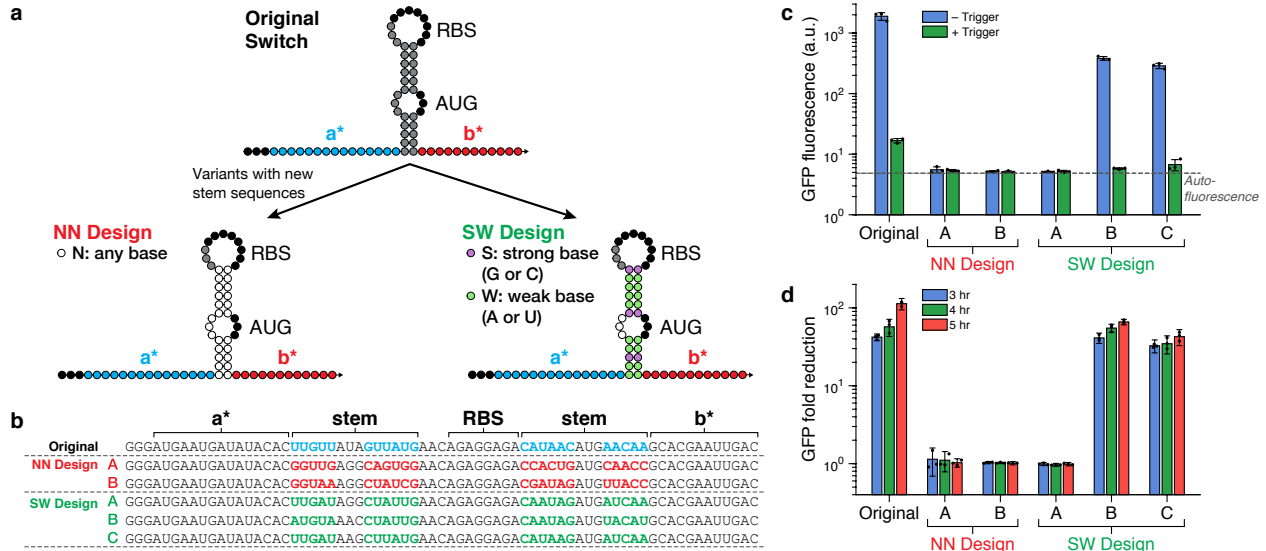
b 3WJ repressor



Supplementary Figure 5 | Characterization of toehold and 3WJ repressors expressed using inducible promoters in MG1655/Marionette-Wild. **a**, GFP fluorescence and fold reduction obtained from first-generation toehold repressor index 1 under various induction conditions. **b**, GFP fluorescence and fold reduction obtained from 3WJ repressor index 19 under various induction conditions. Trigger RNAs were induced by 3OC6-HSL via the P_{luxB} promoter on a ColE1-origin plasmid and switch RNAs were induced by anhydrotetracycline (aTc) via the P_{tet} promoter on a ColA-origin plasmid. The 3WJ repressor requires less trigger RNA to reduce expression than the toehold repressor and is capable of providing over 10-fold GFP reduction within 3 hours even at the lowest 3OC6-HSL concentration tested (0.25 nM). GFP fluorescence values and their errors are the arithmetic mean and SD, respectively, of $n=3$ biologically independent samples. Individual points show fluorescence from $n=3$ biologically independent samples in a (i) and b (i).

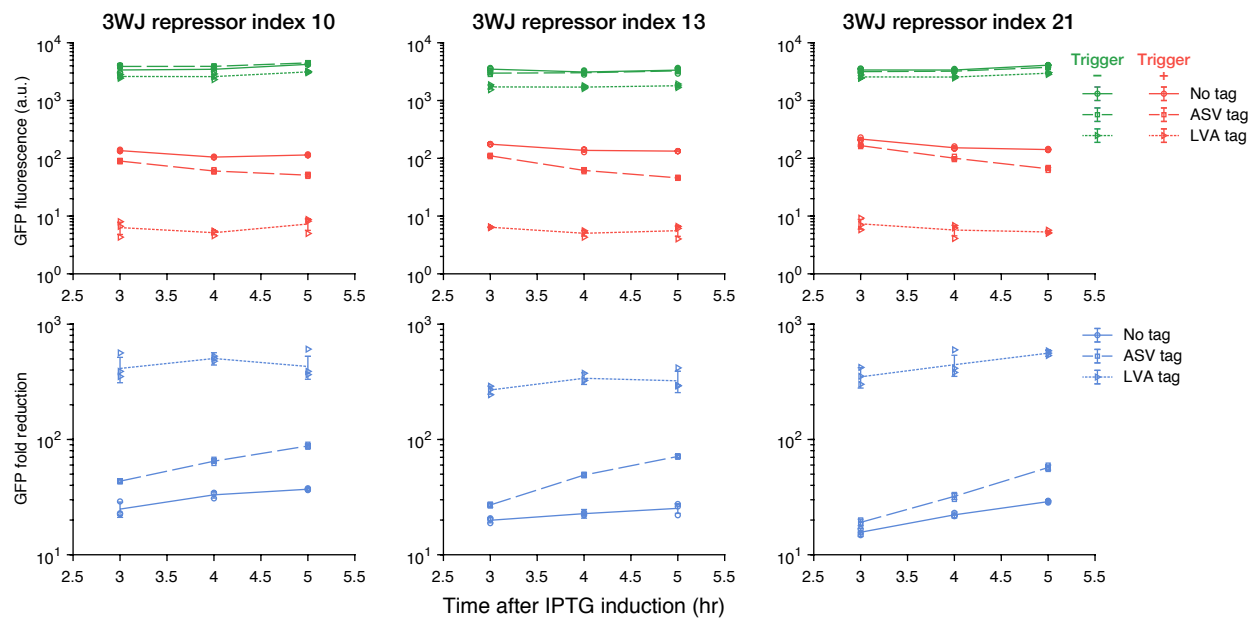


Supplementary Figure 6 | Measurements of toehold and 3WJ repressor performance in cell-free *in vitro* translation reactions. Switch and trigger RNAs for the repressors were transcribed separately *in vitro* and added at known concentration ratios to the cell-free reactions. The levels of GFP translated *in vitro* were then measured over time. GFP fold reduction after 3 hours is shown in the bottom row of plots. Dashed line in the GFP fold reduction plots marks the 10-fold reduction level. For the first-generation toehold repressor index 36 and 3WJ repressor index 20, only a two-fold higher concentration of trigger compared to the switch is sufficient to achieve a 10-fold reduction in gene expression after 3 hours, while four- to six-fold higher trigger RNA is required for the other devices. Individual points show the fluorescence from n=3 technical replicates or the fold reduction from n=3 pairs of technical replicates. In fluorescence plots, lines indicate the arithmetic mean of the fluorescence obtained from n=3 technical replicates. In fold reduction plots, lines show the ratio of the arithmetic mean fluorescence levels of the ON and OFF states.

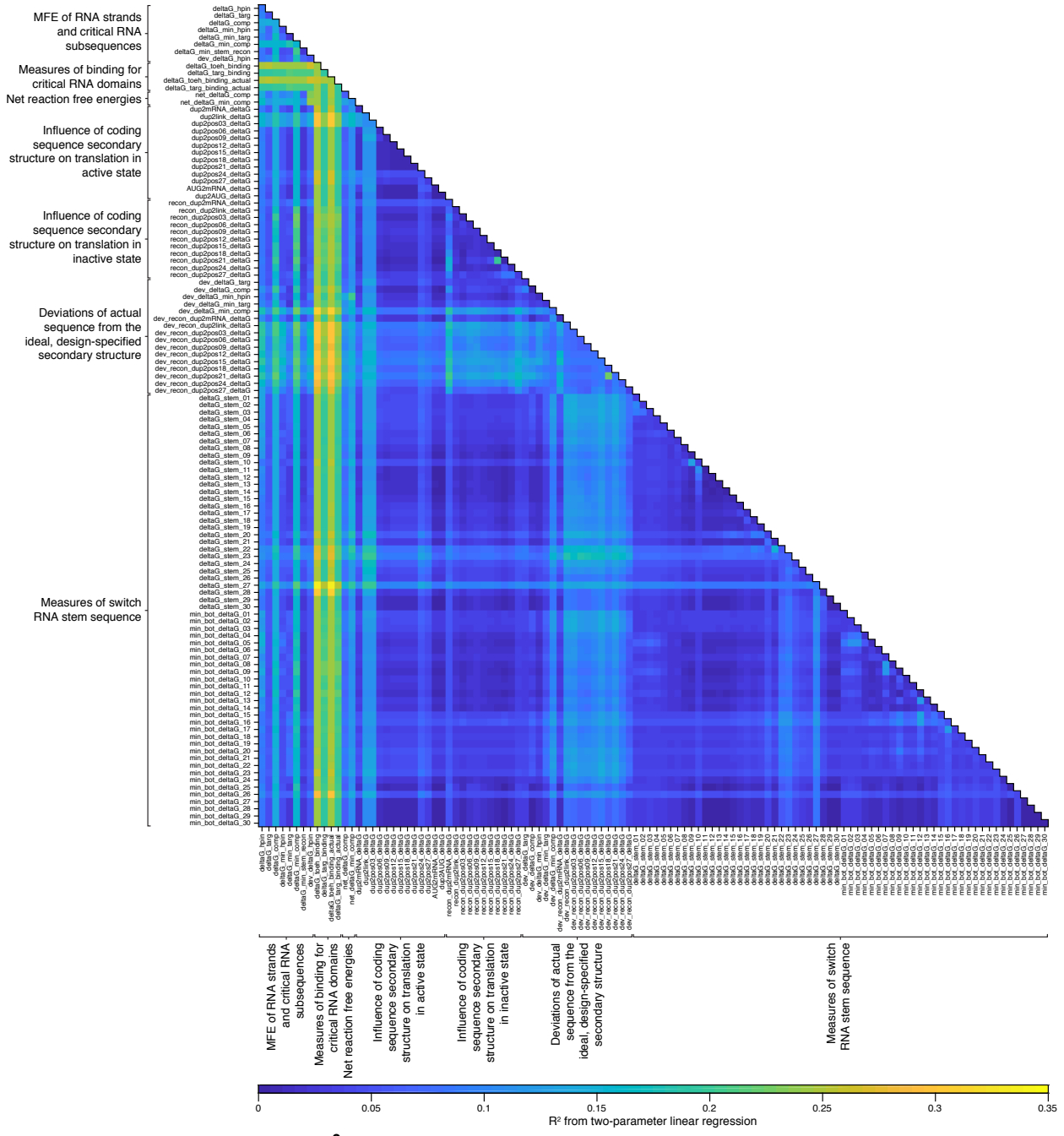


Supplementary Figure 7 | Investigation of 3WJ repressor variants having different sequences in the stem region.

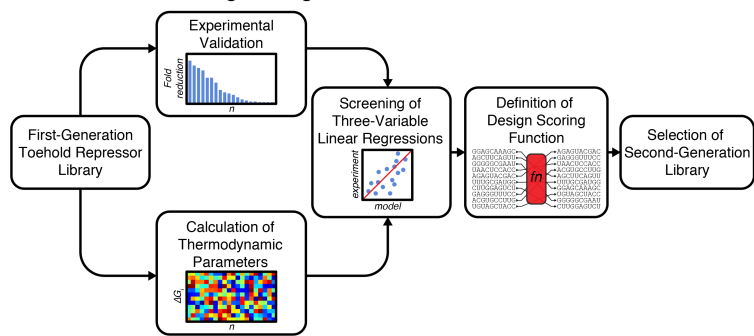
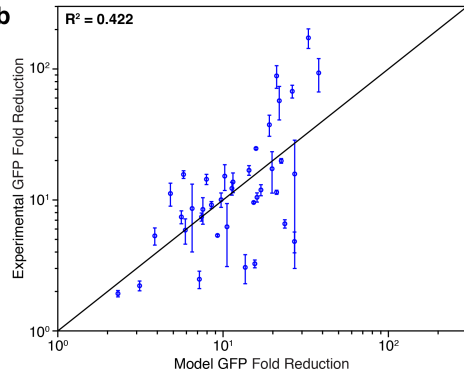
a, Schematic showing the sequence differences incorporated into the NN and SW designs. NN designs use any base (N) in the white positions that satisfy the secondary structure requirements. SW designs retain the same combination of strong (S) and weak (W) base pairs from the original 3WJ repressor design as indicated by purple and green bases, respectively. **b**, Comparison of the sequences used for the original 3WJ repressor index 20 and the NN and SW design variants. Only sequences within the stem region were modified in the variants. **c-d**, GFP fluorescence after 5 hours of induction (c) and GFP fold reduction after 3 to 5 hours of induction (d) measured for the different devices. SW designs B and C with weaker stem secondary structures are able to successfully generate GFP and repress translation in response to the trigger RNA. The two designs also show lower signal leakage than the original repressor. GFP fluorescence values and their error bars are the arithmetic mean and SD, respectively, of n=3 biologically independent samples. Fold reductions for each repressor were calculated by dividing the ON-state fluorescence value by the OFF-state fluorescence value. Relative errors for the fold reductions were obtained by adding the relative fluorescence errors in quadrature. Individual points show the fluorescence measured from n=3 biologically independent samples (c) or the fold reduction (d) from n=3 pairs of biologically independent samples.



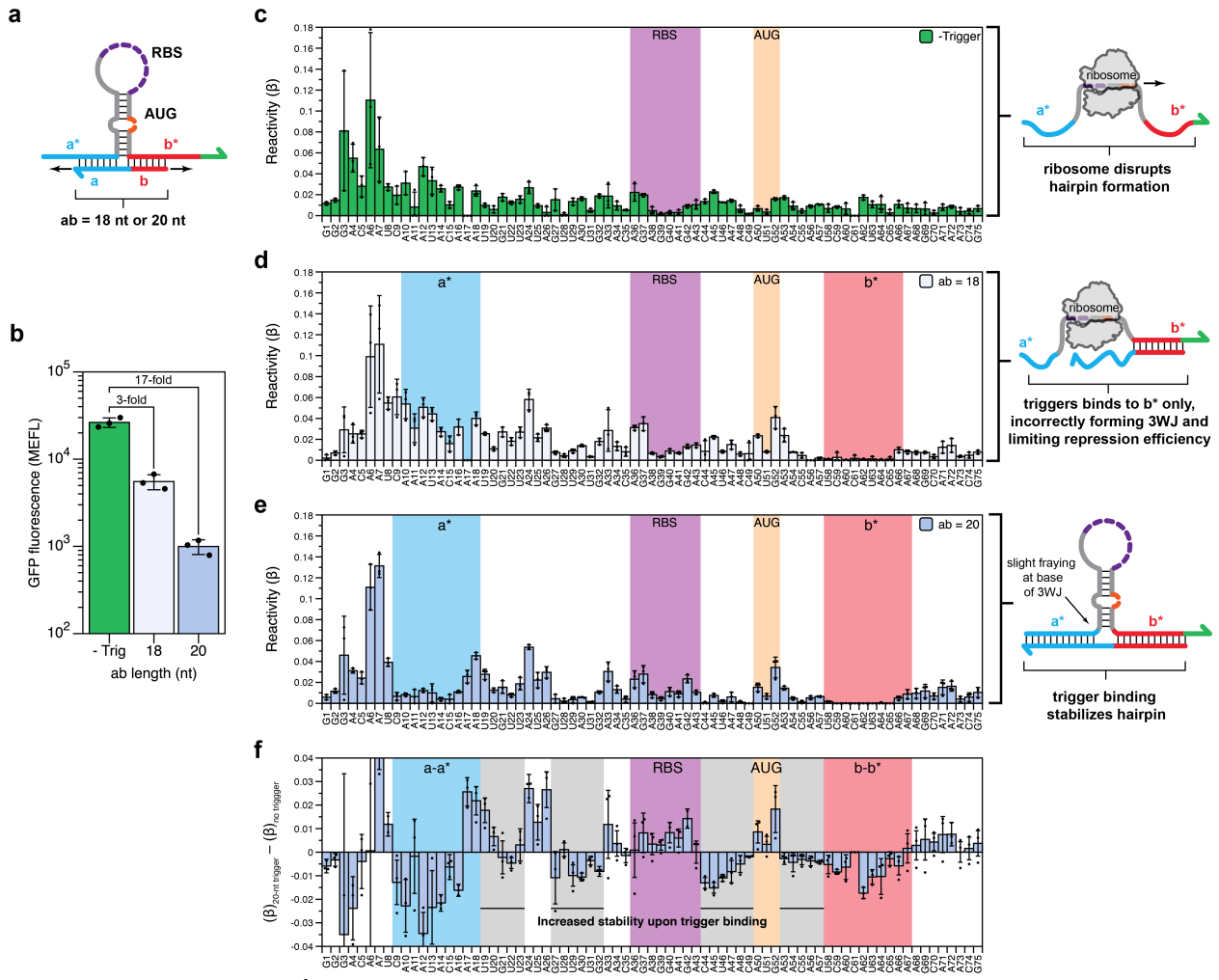
Supplementary Figure 8 | Effect of different degradation tags on 3WJ repressor performance. The GFPmut3b reporter protein was studied with no degradation tag (solid lines, circles), an intermediate-lifetime ASV degradation tag (dashed lines, squares), and a short-lifetime LVA degradation tag (dotted lines, triangles). GFP fluorescence without the trigger (green lines) and with the trigger (red lines) decreased with shorter GFP lifetimes, but a much more pronounced reduction was observed for cases with the trigger present. This effect leads to a significant increase in fold reduction for GFPmut3b-LVA compared to the other GFP variants. GFP fluorescence values and their error bars are the arithmetic mean and SD, respectively, of n=3 biologically independent samples. Fold reductions for each repressor were calculated by dividing the ON-state fluorescence value by the OFF-state fluorescence value. Relative errors for the fold reductions were obtained by adding the relative fluorescence errors in quadrature. Individual points show the fluorescence measured from n=3 biologically independent samples or the fold reduction from n=3 pairs of biologically independent samples.



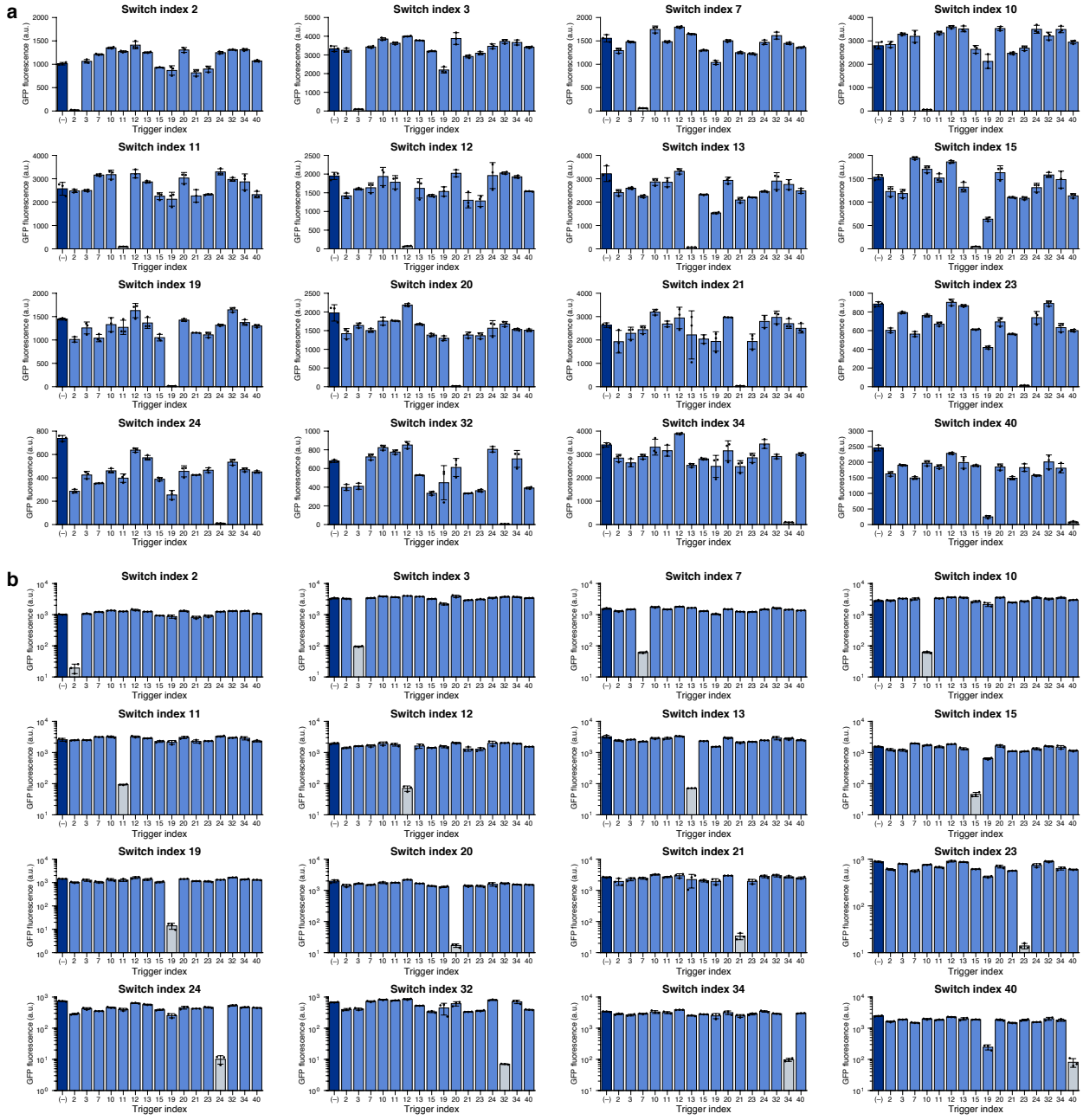
Supplementary Figure 9 | Map of R^2 values of two-parameter linear regressions for the first-generation toehold repressors. Linear regressions were performed on 6,555 combinations of two thermodynamic parameters against the experimental GFP fold reduction values. Hotspots with stronger correlations to device performance can be observed for multiple parameters, such as measures of binding for critical RNA domains.

a Automated Forward Engineering**b**

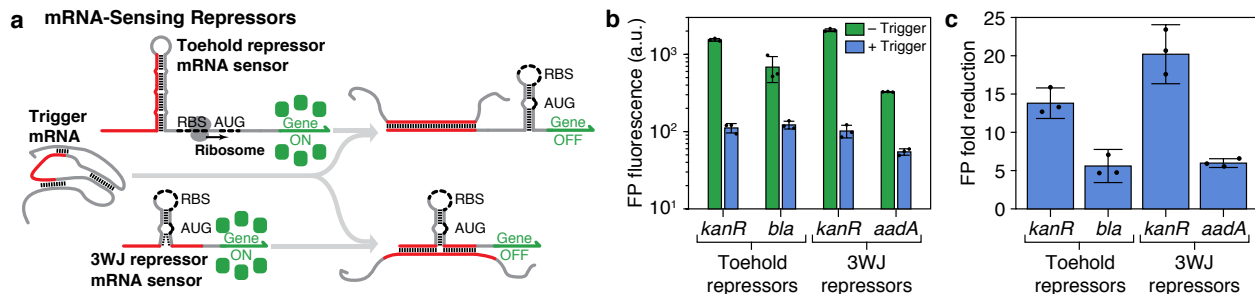
Supplementary Figure 10 | Automated forward engineering of toehold repressors. **a**, Forward engineering was carried out by screening three-variable linear regressions based on 114 different thermodynamic parameters. The top 10 three-variable regressions were used to generate a scoring function, which was then used to select second-generation toehold repressor designs. **b**, Correlation between predicted performance of toehold repressors using a three-parameter linear regression model and experimentally observed performance of the repressors. Experimental fold reduction is the ratio of the mean GFP fluorescence level for the ON and OFF translation states. Relative errors for ON and OFF states are from the SD of $n=3$ biologically independent samples. Relative errors for GFP fold reduction were obtained by adding the relative errors of the repressor ON- and OFF-state fluorescence measurements in quadrature.



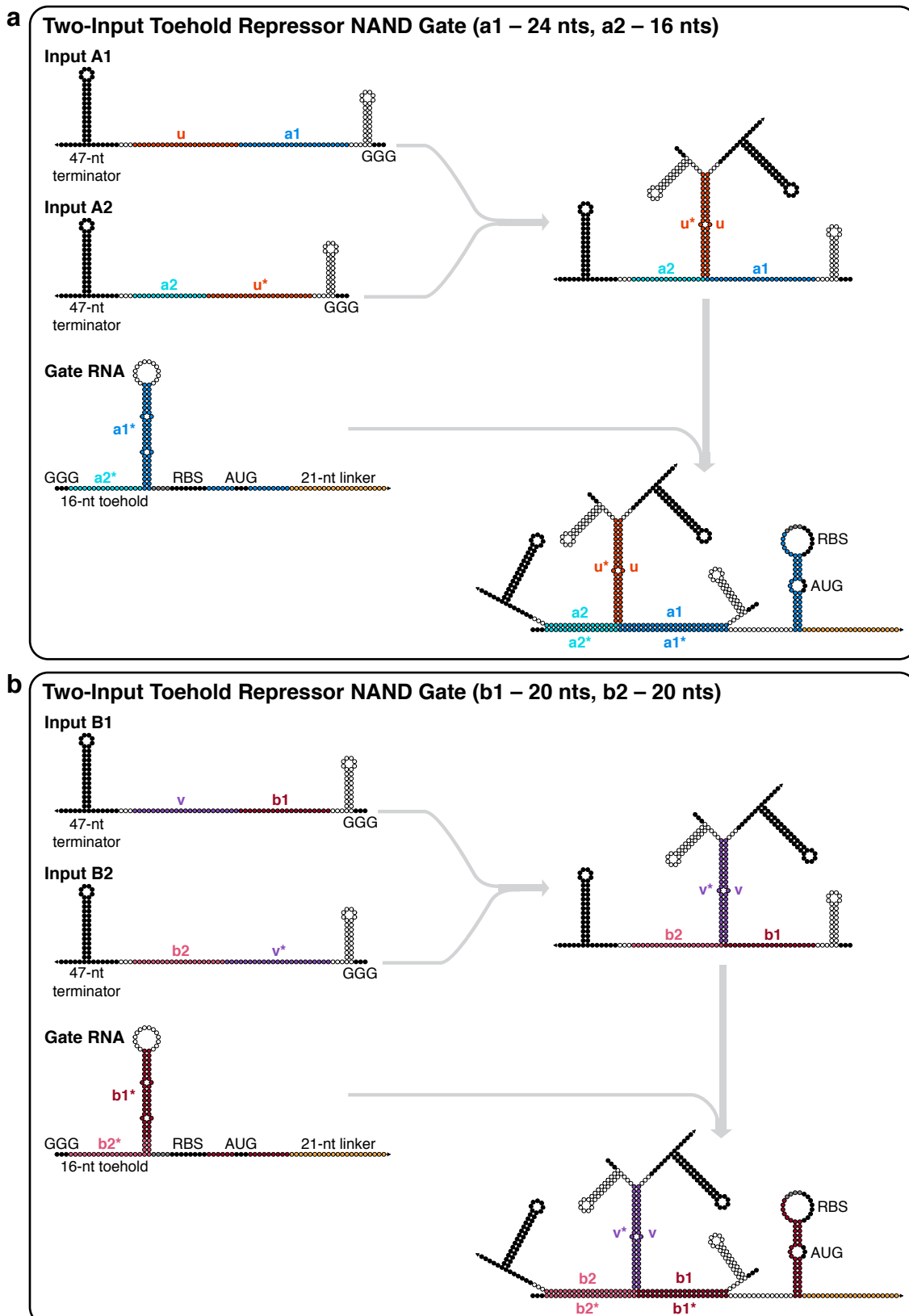
Supplementary Figure 11 | In-cell SHAPE-Seq characterization of trigger variants with varying repression efficiencies. **a**, Design schematic for testing 3WJ repressor variants. A 3WJ repressor switch RNA was characterized using in-cell SHAPE-Seq, either expressed alone or co-expressed with a trigger RNA. Two triggers were tested, with designed binding lengths (**ab**) of 18 nt or 20 nt (see Supplementary Table 7 for sequence information). **b**, Functional characterization of switch RNA expressed without trigger (green) and with triggers of increasing interaction length (blue). Weak repression (fold reduction = 3) is observed when **ab** = 18 nt. Repression efficiency increases dramatically (fold reduction = 17) when **ab** is increased to 20 nt. GFP fluorescence levels and their error bars are the arithmetic mean and SD, respectively, of n=3 biologically independent samples. Individual points show the GFP fluorescence from each sample. **c**, In-cell SHAPE-Seq reactivity profile of the switch RNA expressed alone. A trend of high reactivities is observed across the molecule, consistent with the design hypothesis that the switch hairpin can be disrupted by ribosome binding and actively translated. **d**, In-cell SHAPE-Seq reactivity profile of the switch RNA co-expressed with a poorly-repressing trigger RNA (**ab** = 18 nt). Drops in reactivity are only observed within the **b-b*** interaction domain, suggesting that trigger binding does not occur across the predicted 3WJ. Improper formation of the 3WJ is the likely cause of the weak repression efficiency for this trigger-switch pair, with repression only decreased because of the **b-b*** RNA duplex impeding translation. **e**, In-cell SHAPE-Seq reactivity profile of the switch RNA co-expressed with a longer trigger RNA (**ab** = 20 nt) showing improved repression efficiency compared to the shorter trigger (d). This length variant shows a reactivity profile more consistent with proper 3WJ formation, with reactivity drops observed at the **a-a*** and **b-b*** interaction regions, and within the base-paired stem regions of the switch hairpin. The RBS and start codon (AUG) positions are indicated. For c-e, reactivity levels and error bars represent the arithmetic mean and SD, respectively, of n=3 biologically independent samples. Individual points show the reactivity of each sample. **f**, The difference in reactivities observed between measurements of the 20-nt trigger-switch complex and the switch alone. Relative decreases in reactivity are observed through most of the stem region of the switch with the trigger present (shaded gray), while reactivity increases around the exposed RBS and constrained bulge region of the start codon. Reactivity differences are taken by subtracting the reactivity level in c from the reactivity level in e. Error bars for the reactivity differences were obtained by adding the standard deviations of the reactivity measurements in quadrature. Individual points show the reactivity differences obtained from n=3 pairs of biologically independent samples.



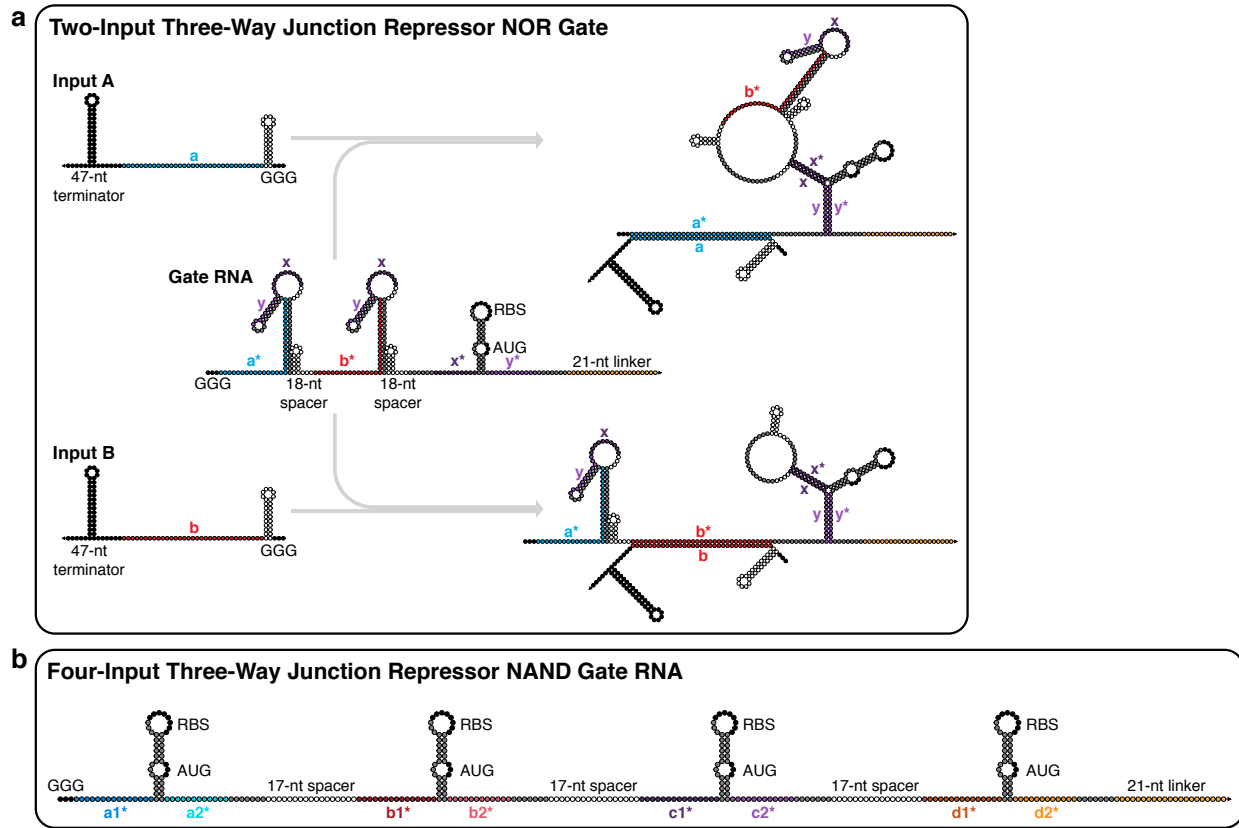
Supplementary Figure 12 | GFP fluorescence levels for 3WJ repressor orthogonality measurements. **a-b,** Linear-scale (a) and logarithmic-scale (b) GFP fluorescence intensities from orthogonality measurements of 16 3WJ repressors after 3 hours of induction. Each switch was tested against the same panel of 17 different cognate (gray bars) and non-cognate trigger RNAs. The non-cognate trigger “(−)” is an RNA with high secondary structure (dark blue bars), while the other non-cognate RNAs are from other 3WJ repressors (light blue bars). Fluorescence levels and error bars represent the arithmetic mean and SD, respectively, of n=3 biologically independent samples. Individual points show the fluorescence from each sample.



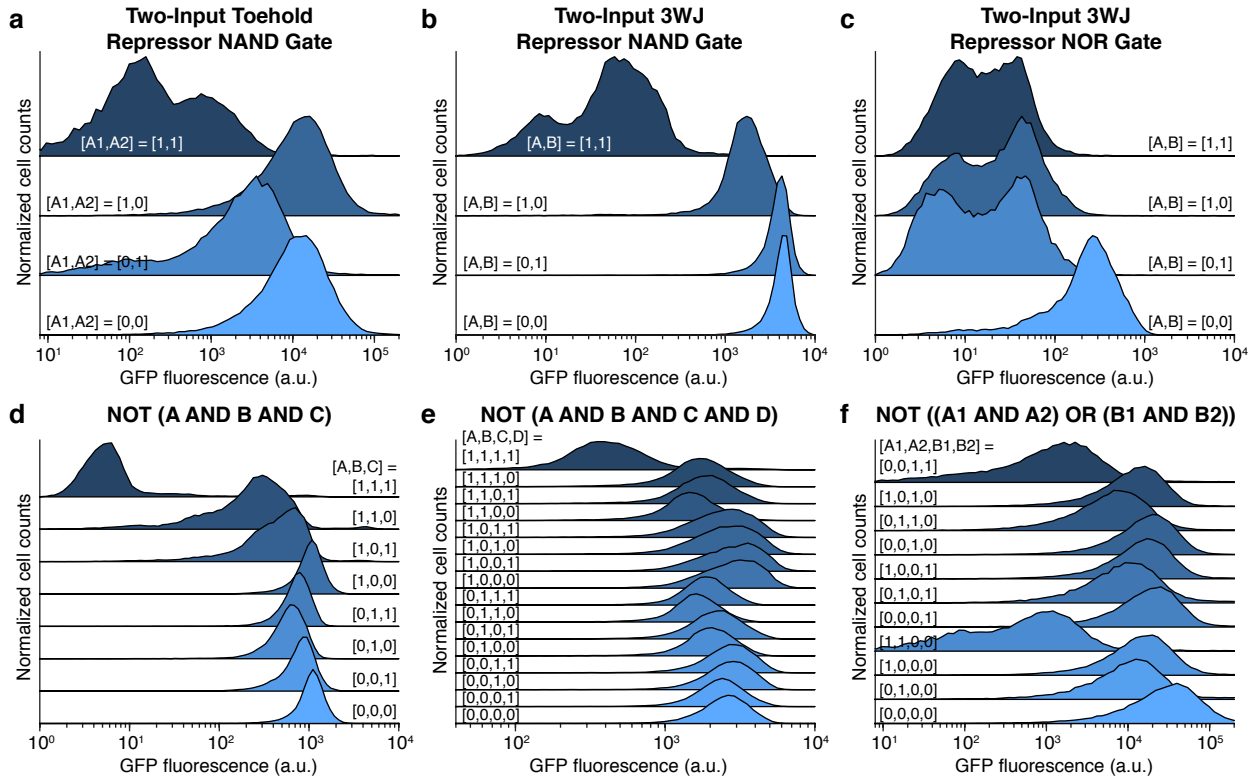
Supplementary Figure 13 | mRNA sensing using toehold and 3WJ repressors. **a**, Design schematic of the mRNA-sensing toehold and 3WJ repressors. The region within the mRNA sequence used to trigger repression is emphasized in red. **b**, Fluorescent protein (FP) fluorescence observed for toehold and 3WJ repressors targeting different pairs of antibiotic resistance mRNAs. **c**, Fold reduction of FP fluorescence for the toehold and 3WJ repressor mRNA sensors. The mRNA sensors used GFP as the reporter, except for the *kanR*-responsive toehold repressor, which output mCherry. Sensors were measured 5 hr after induction. FP fluorescence values and their error bars are the arithmetic mean and SD, respectively, of n=3 biologically independent samples. Fold reductions were calculated by dividing the FP fluorescence value from the switch RNA without the trigger mRNA by the FP fluorescence value obtained with the trigger mRNA. Relative errors are from the SD of three biological replicates. Relative errors for the fold reductions were calculated by adding the relative fluorescence errors in quadrature. Individual points show the fluorescence measured from n=3 biologically independent samples (b) or the fold reduction from n=3 pairs of biologically independent samples.



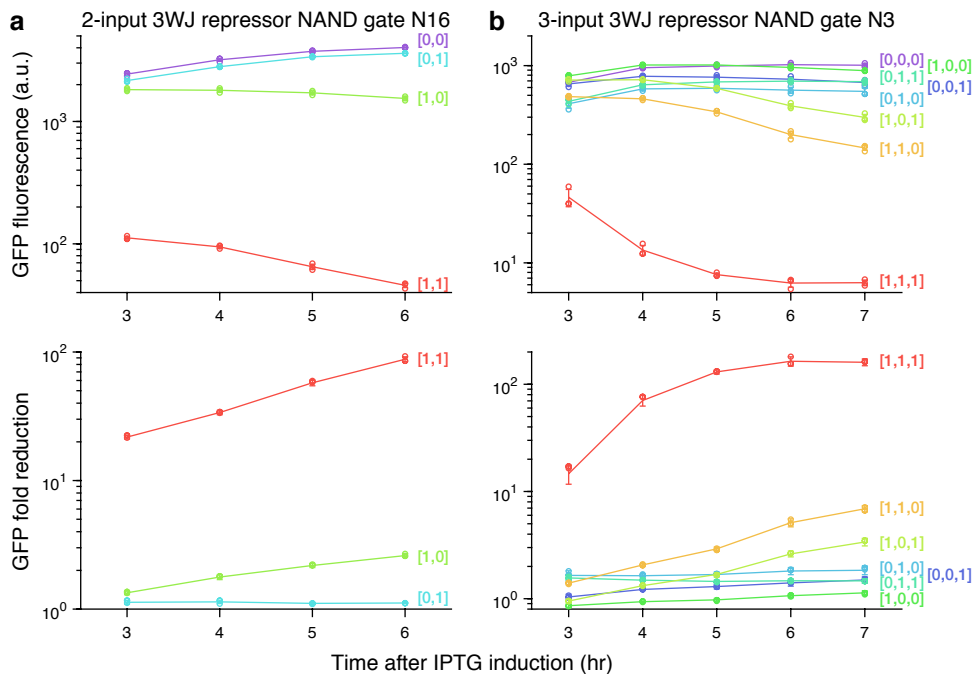
Supplementary Figure 14 | Nucleotide-level schematics for toehold-repressor-based NAND ribocomputing devices. **a-b,** The two-input toehold repressor NAND gate features a modified switch RNA design and employs input RNAs that hybridize through complementary **u-u*** domains (a) and **v-v*** domains (b). The trigger RNA sequence is divided into separate segments of 16 nts and 24 nts each (a) or 20 nts each (b).



Supplementary Figure 15 | Nucleotide-level schematics for 3WJ-repressor-based ribocomputing devices. **a**, The two-input 3WJ repressor NOR gate employs two input-sensing hairpins with loop-confined triggers for a downstream 3WJ repressor hairpin. **b**, The programmed secondary structure for a four-input 3WJ repressor NAND gate RNA. Single-stranded 17-nt spacers separate four 3WJ repressor hairpins and do not encode in-frame stop codons.

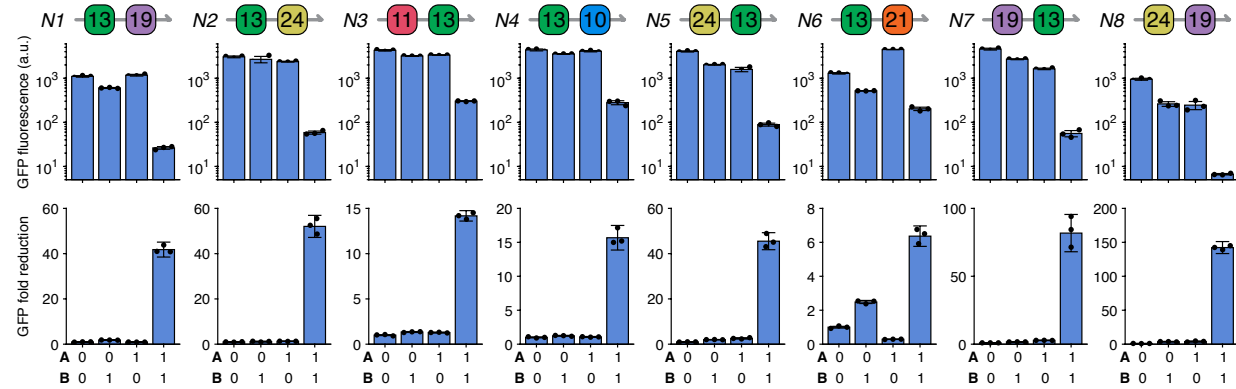


Supplementary Figure 16 | Cell population distributions for ribocomputing logic circuits. **a**, Two-input toehold repressor NAND gate from Figure 5a-c. **b**, Two-input 3WJ repressor NAND gate from Figure 5d-f. **c**, Two-input 3WJ repressor NOR gate from Figure 5g-i. **d**, Three-input 3WJ repressor NAND gate from Figure 6a-c. **e**, Four-input 3WJ repressor NANsD gate from Figure 6d-f. **f**, Toehold repressor NOT ((A1 AND A2) OR (B1 AND B2)) gate from Figure 6g-i. These experiments were repeated n=3 times with biologically independent samples with similar results.

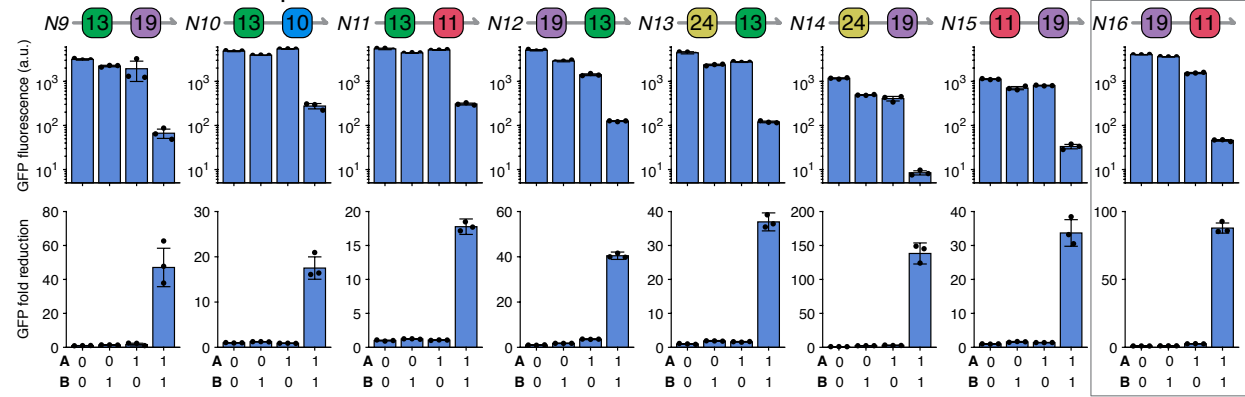


Supplementary Figure 17 | Time-course measurements of ribocomputing devices. **a-b**, GFP fluorescence and fold reduction measured for all input RNA combinations for the two-input (a) and three-input (b) 3WJ repressor NAND gates shown in Figures 5 and 6. GFP expression for the logical TRUE cases generally increases with induction and expression from the logical FALSE cases decreases over time. GFP fluorescence values and their error bars are the arithmetic mean and SD, respectively, of n=3 biologically independent samples. Fold reductions for each device were calculated by dividing the GFP fluorescence value from the gate RNA obtained for the null input case by the GFP fluorescence value for each input combination. Relative errors for the fold reductions were obtained by adding the relative fluorescence errors in quadrature. Individual points show the fluorescence measured from n=3 biologically independent samples or the fold reduction from n=3 pairs of biologically independent samples.

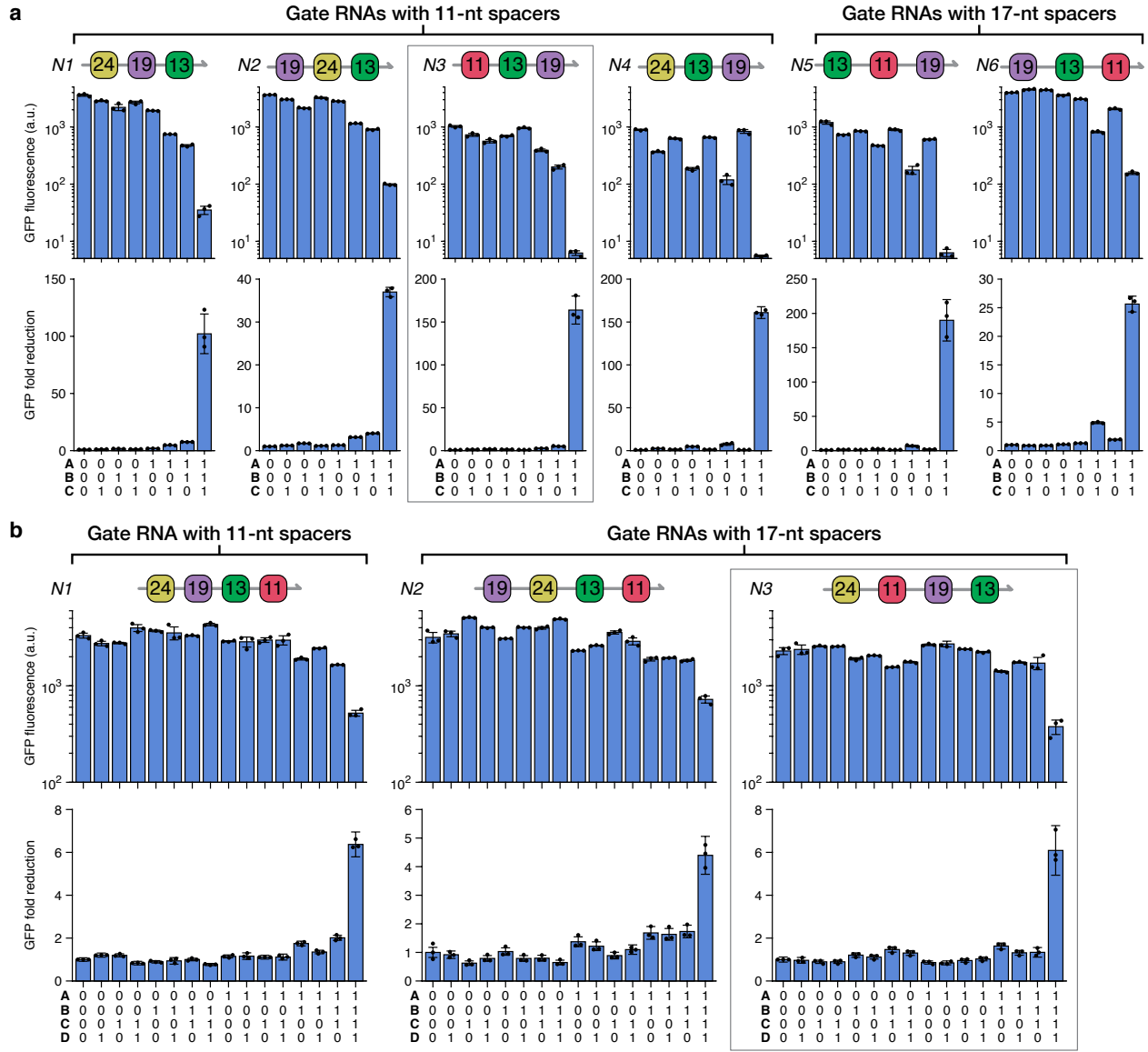
a Gate RNAs with an 11-nt spacer



b Gate RNAs with a 17-nt spacer

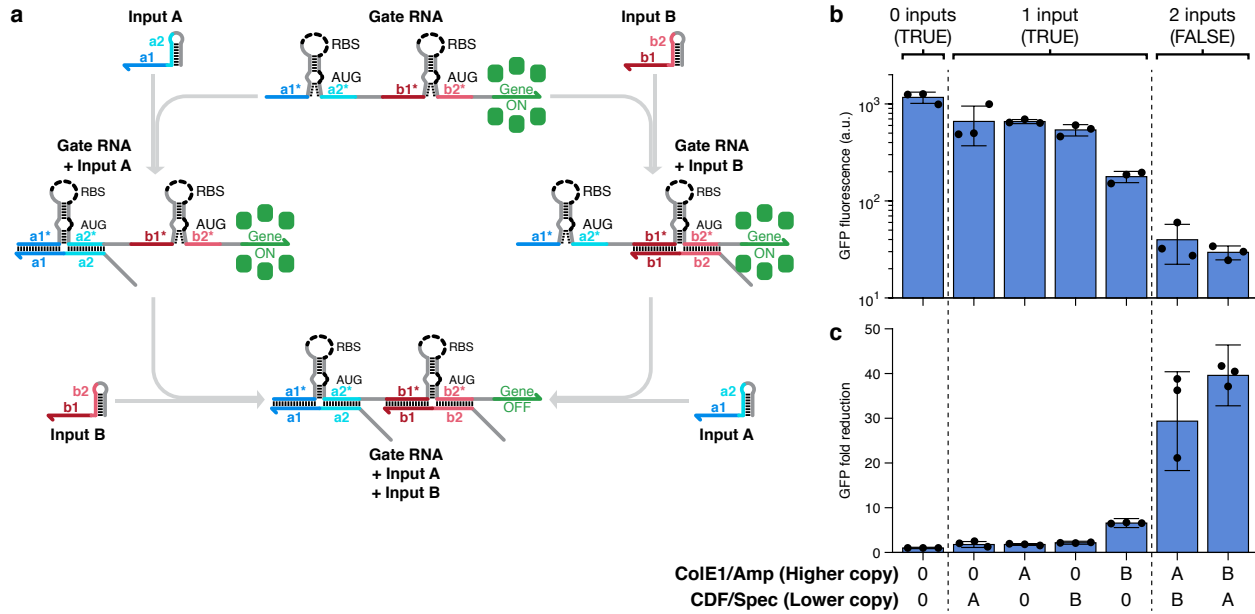


Supplementary Figure 18 | Characterization of 16 different two-input 3WJ repressor NAND gates. **a-b**, GFP fluorescence and fold reduction of eight gate RNAs using an 11-nt spacer between repressor modules (a) and eight gate RNAs using a 17-nt spacer between modules (b). The number of the device and the order and identity of the 3WJ repressor modules used in each gate RNA are listed above the plots. Fourteen out of 16 NAND gates provide at least 10-fold GFP reductions and statistically significant differences between TRUE and FALSE states ($p < 0.023$, unpaired two-sample t-test with unequal variances). Devices N6 and N9 are considered non-functional based on low fold reduction and TRUE state variability, respectively. Device N16 is used in the Figure 5 of the main text as indicated by the gray box. Fluorescence was measured 6 hr after IPTG induction. GFP fluorescence values and their error bars are the arithmetic mean and SD, respectively, of $n=3$ biologically independent samples. Fold reductions for each device were calculated by dividing the GFP fluorescence value from the gate RNA obtained for the null input case by the GFP fluorescence value for each input combination. Relative errors for the fold reductions were obtained by adding the relative fluorescence errors in quadrature. Individual points show the fluorescence measured from $n=3$ biologically independent samples or the fold reduction from $n=3$ pairs of biologically independent samples.

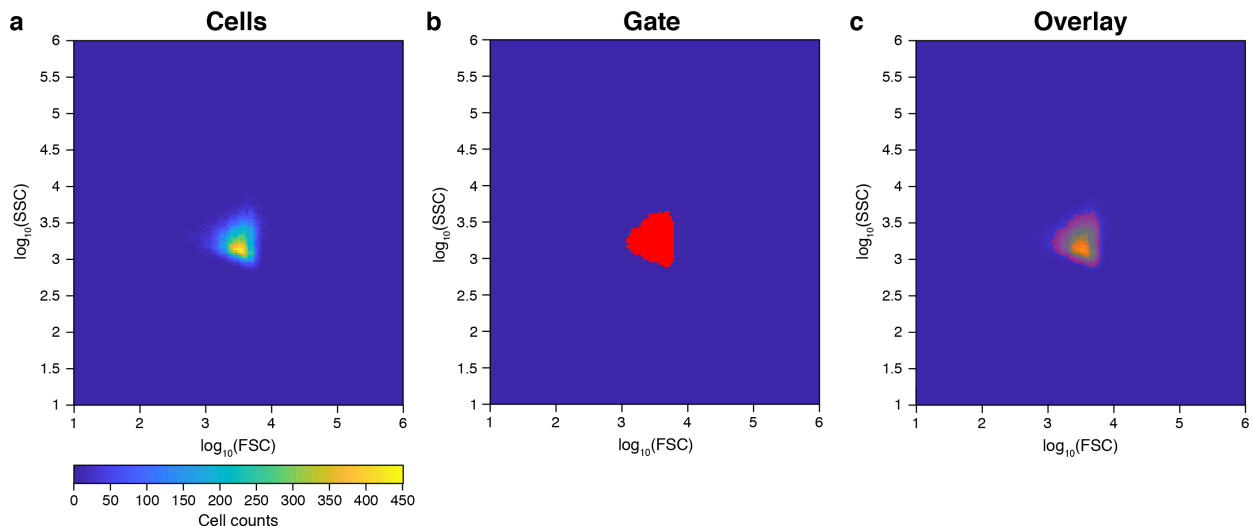


Supplementary Figure 19 | Characterization of different three-input and four-input 3WJ repressor NAND gates.

a-b, GFP fluorescence and fold reduction of six different three-input NAND gate RNAs (a) and three different four-input NAND gate RNAs (b). The number of the device and the order and identity of the 3WJ repressor modules used in the gate RNA are listed above the plots. All three-input and four-input NAND gates provide statistically significant differences between TRUE and FALSE states ($p < 0.016$, unpaired two-sample t-test with unequal variances) and display fold reductions of at least 5-fold and 2.5-fold, respectively. Three-input device N3 and four-input device N3 are used in the Figure 6 of the main text as indicated by the gray boxes. Fluorescence was measured 6 hr after IPTG induction. GFP fluorescence values and their error bars are the arithmetic mean and SD, respectively, of $n=3$ biologically independent samples. Fold reductions for each device were calculated by dividing the GFP fluorescence value from the gate RNA obtained for the null input case by the GFP fluorescence value for each input combination. Relative errors for the fold reductions were obtained by adding the relative fluorescence errors in quadrature. Individual points show the fluorescence measured from $n=3$ biologically independent samples or the fold reduction from $n=3$ pairs of biologically independent samples.



Supplementary Figure 20 | Variations in NAND gate performance based on changes in input RNA plasmid copy number. **a**, Schematic showing different complexes formed between gate and input RNAs depending on the combination expressed. When input B is expressed with the gate RNA, bound input B has the potential to impede translation from the upstream 3WJ repressor module. **b-c**, GFP fluorescence (b) and fold reduction (c) measured for two-input NAND gate N8 using input RNAs expressed from plasmids with different copy numbers in *E. coli* BL21 Star DE3. Weaker translation from the gate RNA is observed when input B is expressed from the relatively higher copy number ColE1-origin plasmid. Fluorescence was measured 6 hr after IPTG induction. GFP fluorescence values and their error bars are the arithmetic mean and SD, respectively, of n=3 biologically independent samples. Fold reductions for each device were calculated by dividing the GFP fluorescence value from the gate RNA obtained for the null input case by the GFP fluorescence value for each input combination. Relative errors for the fold reductions were obtained by adding the relative fluorescence errors in quadrature. Individual points show the fluorescence measured from n=3 biologically independent samples or the fold reduction from n=3 pairs of biologically independent samples.



Supplementary Figure 21 | Gating of flow cytometry data. **a**, Two-dimensional histogram of cell counts as a function of FSC and SSC for a representative population of *E. coli* cells. This histogram was used to define a gate based on values of FSC and SSC where the cell count was at least 10% of the maximum cell count from the peak of the two-dimensional histogram. **b**, The gate generated from the cell population in panel a is shown in red. **c**, Overlay of the gating region over the cell population. The geometric mean fluorescence from the gated cell population was then used for analysis of system performance.

Supplementary Table 1. PCR primers and other sequences used for experiments

Name	Sequence
T7 promoter	TAATACGACTCACTATA[GGG]
Ptet*	TTTCAGCAGGACGCACTGACCTCCCTATCACTGATAGAGATTGACATCCCTATCACTGATAGAGATACTGAGCAC
PluxB	ACCTGTAGGATCGTACAGGTTACGCAAGAAAATGGTTTGTACAGTCGAATAAA
T7 terminator	TAGCATAACCCCTGGGCCTCTAAACGGGCTTGAGGGGTTTTG
Terminator_1	ACTTAAGACGCCGGTCTTGCACCTACCTGCAGTAATGCCGGACAGGATGCCGGTTTCTTCTC
Terminator_2	AGAAAAAAGCCCGCACCTGACAGTGCAGGGCTTTTCGA
Riboj	AGCTGTCACCGGATGTCTTCCGGTCTGATGAGTCCGTGAGGACGAAACAGCCTCTACAATAATTGTTAA
21-nt Linker	AACCTGGCCGCAGCGCAAAG
Switch universal forward primer	GCCGGGTTAGAAATCTGAAGCTCTAGAGAGCGCTAACGACTCACTATAGGG
Switch universal reverse primer	TTACGCATTTGCGCTGCCGCCAGGTT
Trigger universal forward primer	GCCGGGTTAGAAATCTGAAGCTCTAGAGAGCGCTAACGACTCACTATAGGG
Trigger universal reverse primer	CCC GTT AGAGGCCCAAGGGTTATGCTA
Switch backbone forward primer	AACCTGGCCGCAGCGCAA
Switch backbone reverse primer	TCTCTAGAGCTTCAGATTCTAAACCCGGCCATAAGGGAGAGCGTCGAGATC
Trigger backbone forward primer	TAGCATAACCCCTGGGC
Trigger backbone reverse primer	TCTCTAGAGCTTCAGATTCTAAACCCGGCCAGATCTCGATCCTCTACGC
Non-cognate RNA used for library characterization	GGGUUCUACGCCUCAGCUGGGCGUGAGAUGAGCCUCGUCCAGAUGACGAGGCAACGUAGGAUCUGACUGAUCCUAU
GFPmut3b-ASV	ATGCGTAAAGGAGAAGAACCTTCACTGGAGTTGCCAATTCTGTTGAATTAGATGGTATGTTAACGGCACAAATTCTGTCAGTGGAGAGGGTGAAGGTG ATGCAACATACGGAAAACTTACCCCTAAATTATTGCACACTGGAAAACTACCTGTTCCGGCCAACACTTGTCACTACTTCGGTTATGGTGTCAATGCTT GCGAGATACCCAGATCACATGAAACAGCATGACTTTCAAGAGTGCCATGCCGAAGGTTACGTACAGGAAAGAACTATATTCAAAGATGACGGGAACTA CAAGACACCGTGTGAAGTCAAGTTGAAGGTGATACCCTGTTAATAGAACGTTAAAGGTTATTGATTAAAGAAGATGGAACATTCTGGACACAAATTG GAATACAACATAACTCACACAATGTATACTCATGGCAGACAAACAAAAGAATGGAATCAAAGTTAACTCAAATTAGACACAAACATTGAAGATGGAAGCGTTC AACTAGCAGACCATTATCAACAAAATCTCGATTGGCGATGCCCTGTCTTACAGACAACCATTACCTGTCCACACAATCTGCCCTTCGAAAGATCCC AACGAAAAGAGAGACCACATGGCCTCTTGAGTTGTAACCGCTGGGATTACACATGGCATGGTGAACATACAAAAGGCCTGCAGCAAACGACGAAAA CTACGCTGCATCAGTTATAA
GFPmut3b-LVA	ATGCGTAAAGGAGAAGAACCTTCACTGGAGTTGCCAATTCTGTTGAATTAGATGGTATGTTAACGGCACAAATTCTGTCAGTGGAGAGGGTGAAGGTG ATGCAACATACGGAAAACTTACCCCTAAATTATTGCACACTGGAAAACTACCTGTTCCGGCCAACACTTGTCACTACTTCGGTTATGGTGTCAATGCTT GCGAGATACCCAGATCACATGAAACAGCATGACTTTCAAGAGTGCCATGCCGAAGGTTACGTACAGGAAAGAACTATATTCAAAGATGACGGGAACTA CAAGACACCGTGTGAAGTCAAGTTGAAGGTGATACCCTGTTAATAGAACGTTAAAGGTTATTGATTAAAGAAGATGGAACATTCTGGACACAAATTG GAATACAACATAACTCACACAATGTATACTCATGGCAGACAAACAAAAGAATGGAATCAAAGTTAACTCAAATTAGACACAAACATTGAAGATGGAAGCGTTC AACTAGCAGACCATTATCAACAAAATCTCGATTGGCGATGCCCTGTCTTACAGACAACCATTACCTGTCCACACAATCTGCCCTTCGAAAGATCCC AACGAAAAGAGAGACCACATGGCCTCTTGAGTTGTAACCGCTGGGATTACACATGGCATGGTGAACATACAAAAGGCCTGCAGCAAACGACGAAAA CTACGCTTAGCTTATAA
GFPmut3b-notag	ATGCGTAAAGGAGAAGAACCTTCACTGGAGTTGCCAATTCTGTTGAATTAGATGGTATGTTAACGGCACAAATTCTGTCAGTGGAGAGGGTGAAGGTG ATGCAACATACGGAAAACTTACCCCTAAATTATTGCACACTGGAAAACTACCTGTTCCGGCCAACACTTGTCACTACTTCGGTTATGGTGTCAATGCTT GCGAGATACCCAGATCACATGAAACAGCATGACTTTCAAGAGTGCCATGCCGAAGGTTACGTACAGGAAAGAACTATATTCAAAGATGACGGGAACTA CAAGACACCGTGTGAAGTCAAGTTGAAGGTGATACCCTGTTAATAGAACGTTAAAGGTTATTGATTAAAGAAGATGGAACATTCTGGACACAAATTG GAATACAACATAACTCACACAATGTATACTCATGGCAGACAAACAAAAGAATGGAATCAAAGTTAACTCAAATTAGACACAAACATTGAAGATGGAAGCGTTC AACTAGCAGACCATTATCAACAAAATCTCGATTGGCGATGCCCTGTCTTACAGACAACCATTACCTGTCCACACAATCTGCCCTTCGAAAGATCCC AACGAAAAGAGAGACCACATGGCCTCTTGAGTTGTAACCGCTGGGATTACACATGGCATGGTGAACATACAAAAGGCCTGCAGCAAACGACGAAAA CTACGCTTATAA

Supplementary Table 2. Sequence and performance information for first-generation toehold repressors

NOTES:

1. Trigger RNA sequences are listed up to the base immediately before the T7 terminator used to terminate transcription.
 2. Switch RNA sequences are listed up to the 30th base (inclusive) following the end of their trigger binding domain. This 30-nt sequence contains the 21-nt linker sequence and the first 9-nts of GFPmut3b.
 3. Devices were measured 3 hr after induction. GFP fluorescence values and their errors are the arithmetic mean and SD, respectively, of n=3 biologically independent samples. Fold reductions for each device are calculated by dividing the GFP fluorescence value from the ON state by the GFP fluorescence value from the OFF state. Relative errors for the fold reductions were obtained by adding the relative fluorescence errors in quadrature.

First-generation toehold repressor ranking	First- generation toehold repressor index	GFP fold reduction	Switch sequence	Trigger sequence	Switch plasmid	Switch plasmid origin/Resistance	Trigger plasmid	Trigger plasmid origin/Resistance
1	9	172.8 ± 29.4	GGGAAAGUGAAGAAGAAUAUAAGUUGAAGGAAGGCAGAUGAUUGUAAGGU UACUACACUUACACUCACUGCJUUCAUUCUACUUUAACAGAGGGAGA AUAAAAGAUGAAGAACCGAACCUCCGGCGCAGCGCAAAGAUGCGUAAA	GGGUCAAGGCAUUAGCCCUAUGCCUJG AAUACUUAACAUCAUCGCCJUCAUUCAA CUUUUAUACUUCUUCACUUUACU	pAG_ToeRep_N09_switch	ColA/kanamycin	pAG_ToeRep_N09_trigger	CDF/spectinomycin
2	40	93.3 ± 26.6	GGGAAUAAAAGAAAGAUGAAUAUAUGUGAAGAUAAGGUUGAUGAAUGUAUA CUUAAUUAACAUUUAACCUUACUUCUCAUJUUAACAGAGGGAGA UAAAUAUGAAGAACCGAACCUCCGGCGCAGCGCAAAGAUGCGUAAA	GGGAGUCGGUCUCGCCGUJGAGACCGA CAUUCUACAUCAUCACCUCUACU CAUUCUACUUCUUCUUUAUACU	pAG_ToeRep_N40_switch	ColA/kanamycin	pAG_ToeRep_N40_trigger	CDF/spectinomycin
3	1	88.5 ± 17.4	GGGAGAAAUGAAGAUAAGAUAGUGUGAUGAGUGCGAGUUGUUAAC AAAUAACUUAACUUCUJCUGCUCUCAUCUAAACAGAGGGAGA UAGAUUAUGAAGAGCAACCUGCGCGAGCGCAAAGAUGCGUAAA	GGGUCAGACAACCGGUJGAGGUUJGUCUG AAUUAUUAACAUUCUCCACUACU AUCUACUUCUACUUCUAC	pAG_ToeRep_N01_switch	ColA/kanamycin	pAG_ToeRep_N01_trigger	CDF/spectinomycin
4	42	67.5 ± 7.5	GGGAGAAUAAAAGAGAAUAGAGGUGAGAAGAACGGUGAAGAAUUAUC AACAUUAUUAUUCUCCACCGUUCUUCUCGCUCUAAACAGAGGGAGA AUAGAGAUGAAGAACGAAACCUCCGGCGCAGCGCAAAGAUGCGUAAA	GGGCGAACUUGAAACAGGGAUJCAAGUUC GCAUUAUUCUUCUUCACCGUUCUUCUCA CCUCUACUUCUUCUUUAUACU	pAG_ToeRep_N42_switch	ColA/kanamycin	pAG_ToeRep_N42_trigger	CDF/spectinomycin
5	36	57.2 ± 16.4	GGGAGAAUAAAUGAGGAGAUAGAGGUGAGAUGAGGAGAGUGAGUAGUA CAAUAACACUACUACUCCUACUUCUCAUCUAAACAGAGGGAGA UAGAGAUGAAGAGAACCGAACCUCCGGCGCAGCGCAAAGAUGCGUAAA	GGGCUUJGACUGAUGCAACGAGUCAAG GCAAACUACUACACUCCUCAUCUCCA CUCUACUCCUCAUUAUACU	pAG_ToeRep_N36_switch	ColA/kanamycin	pAG_ToeRep_N36_trigger	CDF/spectinomycin
6	25	37.5 ± 6.9	GGGAGAAAUGAAGAUAAGAAAUGAGAGAACGGGAAUAJAAAGAAC UUACUACUUUAUUAUUCGUUCUCACUUCUUAUAACAGAGGGAGA UAAGAAUGGAGAGAACGAAACCUCCGGCGCAGCGCAAAGAUGCGUAAA	GGGUUGGAGUACGAGCGAGUUCUAC CACGACUUUAUUAUUCGGUUCUCA UUUCUUAUCAUCUUCUACUUUUCU	pAG_ToeRep_N25_switch	ColA/kanamycin	pAG_ToeRep_N25_trigger	CDF/spectinomycin
7	35	24.7 ± 0.5	GGGAAGAGAUGAGAGAAUAGAAGUGGUGGGAUJGGGAGGUGUGUUA CAAUGAAUUAACGAGCGCACCUACUUAUUAUCAUAAACAGAGGGAGA AUAGAAUAGAAGAGAACCGAACCUCCGGCGCAGCGCAAAGAUGCGUAAA	GGGUCAUGGGACUUGAUUCCUACU GAAUAAAACGCGCACCACAUJAC AUUCUACUUCUCAUCUACUUAU	pAG_ToeRep_N35_switch	ColA/kanamycin	pAG_ToeRep_N35_trigger	CDF/spectinomycin
8	6	19.9 ± 0.8	GGGAAAGAUGGAGAAGAAUAUAUGAGGGAGGGAUJGGGAGGUGUGUUA GAAACAGAUACACAAACCUCCUACUCCUCCAUCAUAACAGAGGGAGA AUAGAUUAUGAGGGAUAGAACCUCCGGCGCAGCGCAAAGAUGCGUAAA	GGGCGGCAGAUGCUAGUCAGCAUCUGC CGCAAUACACACACCUCUCCAU CAUCUUAUACUUCUCCAUUUAAU	pAG_ToeRep_N06_switch	ColA/kanamycin	pAG_ToeRep_N06_trigger	CDF/spectinomycin
9	21	17.3 ± 6.0	GGGAAAGAAUAGAUAAGAAUAUAUGAUAUGGCGCUGUAUGUGUUGUAC GGAAGAGACAAACAGAUACAGCUCCAUUCAUUAACAGAGGGAGA UAUAAAUGGAUAGGAGAACCGAACCUCCGGCGCAGCGCAAAGAUGCGUAAA	GGGUUCGGGAUGCUUGGUAGCAUCCCA GAGAACACACAUACAGCGCAAUCAU CAUUAUACUUCUACUUAU	pAG_ToeRep_N21_switch	ColA/kanamycin	pAG_ToeRep_N21_trigger	CDF/spectinomycin
10	3	16.8 ± 1.4	GGGAGUGAAAGAGUGAAGAUAAGAGGUGAGAGUGGAUGUGUGUGAGA ACAAGAACUACAAACAUCCUACUCUCAGCUCUUAUAACAGAGGGAGA AUAAAUGGAGAGAGAACCUCCGGCGCAGCGCAAAGAUGCGUAAA	GGGCGGCCAGGUGCGAAGUGGACCU CGCAGCUACACACACUCCACU CUCUUAUACUUCUUCUACUUUA	pAG_ToeRep_N03_switch	ColA/kanamycin	pAG_ToeRep_N03_trigger	CDF/spectinomycin
11	13	15.8 ± 12.8	GGGAAGAUAGAAGAAUAUAAGAAUAGAAGAACGUGUAGAAUAGUCA UAACAAACUUAUUAUACGUUUCAUCACUCUUAUAACAGAGGGAGA UAAGAGUGGAUGAAACGAAACCUCCGGCGCAGCGCAAAGAUGCGUAAA	GGGAGGUGCGAAUCUCAAGAAUUCG CAAAUCUACACACAGCACU CUUUUAUACUUCUACUUAU	pAG_ToeRep_N13_switch	ColA/kanamycin	pAG_ToeRep_N13_trigger	CDF/spectinomycin
12	34	15.6 ± 1.1	GGGAUAAAUGGAAGGAGGUAAAAGGGUGGAGAGUGCGUGUGUUGAG ACAUAUUAUACUCAAGACACAGCUCUCUCCACCUUUAUAACAGAGGGAGA AUAAAUGGAGAGAGAACCUCCGGCGCAGCGCAAAGAUGCGUAAA	GGGCCACGUUAUGAAUCGCCAUACUG GCAAAUCUACACACAGCACU CUUUUAUACUUCUCCAUUAU	pAG_ToeRep_N34_switch	ColA/kanamycin	pAG_ToeRep_N34_trigger	CDF/spectinomycin
13	26	15.2 ± 3.4	GGGAAUJGGAGAGAAGUGAAGAGAAUAGAGGAUAGGCGAUGAAUAGAU ACCUUUAUACUCAUUAUACGUUUCAUCACUCUUAUAACAGAGGGAGA AUAGAAAUGAAGAGACGAAACCUCCGGCGCAGCGCAAAGAUGCGUAAA	GGGUCCGGUUAAACGCCAUUACCG ACAUACUACUUCUACUGCCU UUCUACUACUUCUCCAUUAU	pAG_ToeRep_N26_switch	ColA/kanamycin	pAG_ToeRep_N26_trigger	CDF/spectinomycin

14	20	14.4 ± 1.3	GGGAGAAGUGAGGGAGGGUAAGAGGGAGUAUGGGCGGAGUGAGUAC ACACAAUUAACACAUCACCCGCUUACUCUCUCUUAUAACAGAGGGAGA AUAGAAAUGAGUAAGAGCAACCUGGCCAGCGCAAAGAUGCGUAAA	GGGCCUUGGUAGAAUACCCUCUACACAG GCAUACUACACUCACCGGCACUUACUCCC UCUUAUCCACUCCUCACUUCUUA
15	27	13.7 ± 2.4	GGGAUGGAGAGAGAGAGUAAGAGUGAGAGGGCGUJUUGAGUAGUA AUAGAGAACACUAACACGUCUCUCAACUUAUAACAGAGGGAGA AUAAAAGAUGAGAGAGACGAACCUGGCCAGCGCAAAGAUGCGUAAA	GGGUCCGAUAGCUCAGAUAGCUAUCCG ACAAACUACUCAACACGCCUUCUACA CUUUACUCAUCUCUCCUCAUUAU
16	33	12.3 ± 1.4	GGGAGAAGUGGAGAAGUAAGGGAGAUGAGGGAGAGUGAGUAAGG ACAUACAAUUAACACUCCUCAUCUUCUCAUUAACAGAGGGAGA AAUGAAAUGAAGAUGAGGAACCUGGCCAGCGCAAAGAUGCGUAAA	GGGCGUGGUUACGGGUUGGCCUGAACCA CGCAAUUACUACUCUCCUCAUCUUC CCUUCAUACUUCUCCACUUUCAUA
17	8	11.9 ± 1.2	GGGAGAAGUGAUAGAAGAAUUAUGGUAAAGAGUGCAGGUUGUUGUAUGA ACCUGGAUACACACUCUGCUCUUAACUUAUAACAGAGGGAGA UAUAUAUGAAGAGAGCAACCUGGCCAGCGCAAAGAUGCGUAAA	GGGAGUGACGGUGUGGCAACCGGUCA CUAAUUAUACAAACACUCGACUUCUJAC CUAUUAUUCACUCAUACUUCUUA
18	28	11.4 ± 0.4	GGGAUGAAGAUAGAAAAGUAAGGGUGAGAAUAGGAGAGAGUAAGUUC AAUUCACUUAUACUCUCCAUUCUCAACCUUUAACAGAGGGAGA AUAAAAGAUGGAGAAUAGGAACCUGGCCAGCGCAAAGAUGCGUAAA	GGGCGAGUGCCUUUAGACAAAGGCACUC GCAUACUUAUCUCUCCUCAUUCUAC CCUUUAUCUUUCAUCUCAUCUCAU
19	37	11.2 ± 2.2	GGGUUGGAAAGUGGAGGAGAUGAAGAGGAUAGGGUGGUAGUAGUA CGAACCAACACUACUACACCUCUCCAUUCUCAUUAACAGAGGGAGA AUUGAAAUGGAUAGGGAGGAACCUGGCCAGCGCAAAGAUGCGUAAA	GGGUCAUACCCUCGCGAAUGAGGGUAG ACAAACUACUACACCUCUCCAUUCU UUCAUCUCCUCAUCUCAUUAU
20	5	10.5 ± 0.8	GGGAGAAGUGGAAGAGUGUAAGAGGGUGAGAUGGGUUGAGGAGUUGUA ACGACUCGACAAACUACUACCUACUGCUCUUAACAGAGGGAG AAUAAGAAAUGGAGAUGAGGAACCUGGCCAGCGCAAAGAUGCGUAAA	GGGCGCAAUUAUACUGUCAUGGUUAUUGC GCAAAACACUCCUCAACCAACUUC UCUUAUCACUCUCCACUUCUUA
21	22	10.0 ± 1.3	GGGAGAAGUAAGAGAGUGAUUAAGUGUGUGAUGUCGGUUGUGCUUUA ACGAAACAAUUAAGAACACCGUCAUCACUACUUAACAGAGGGAGA UUAGAUGGUGAUGAGCAACCUGGCCAGCGCAAAGAUGCGUAAA	GGGCCUUUCUGGGCAUGGUCCCAAG GGAAUUAUAAAGCACACCGACAUACACA UCUUAUCACUCUCCACUUCUUA
22	41	9.6 ± 0.2	GGGAAGUGAAGAAGAUAAAGAGUGAAGAGCGUGUAGUAAGUACC UACUACUACUUAACAGCUUCUUCACUUCUUAACAGAGGGAGA AUAAAAGUAGGAGAAAGCAACCUGGCCAGCGCAAAGAUGCGUAAA	GGGUCCUGGACGUAGUUUUGUACGUCA GAUUAUACUUUACACAGCCUUC UCUUAUCACUUCUCAUCUUAU
23	44	9.5 ± 0.5	GGGAUUAAGAGAUGGGAGUAAGGGUGGAGAGGGUGAGAGAAC UACAUACUUCUCAUACCCUUCUACUCCUUUAACAGAGGGAGA AUAAAAGUAGGAAAGUAGGAACCUGGCCAGCGCAAAGAUGCGUAAA	GGGCGCUACAGAACCCGUCCGUUC CGCAUUCUCCUACCCCCACUUC CCCUUUAUCUCCACUUCUUAU
24	11	9.2 ± 0.6	GGGAGGAUGGAGAGAAUUAAGAGGGUGGGUGGUUGGUAGUUC AGAACAAUUAACACUACCCUCCUACAGCUUCAUAAACAGAGGGAGA AUAGAAAUGGAGGGCAGGAACCUGGCCAGCGCAAAGAUGCGUAAA	GGGACACUAGCCGUUCGAUCGGCUAGU GUCGAAUUAACUACUACACCAGCCU CUUCUAAUUCUCCACUUCUUAU
25	23	8.6 ± 4.6	GGGCGUGAGCGGAUGAAUUAAGUGUGUAAGUGGUGUGAUGUAGUA CGACGACAUACUACUACACCUCUUAUCUCAUUAACAGAGGGAG AUAGAAAUGAUAAAAGGAGAACCUUGGCCAGCGCAAAGAUGCGUAAA	GGGAGLUUACACAGGUGCGUUGUACAC UAAAACUACAUACACCCACUUAU AUCUUAUUCUCCACUACGAAC
26	4	8.5 ± 1.9	GGGAUUGGAGAGAGUGGGAGAGUGUGAGGGAGUGCGAAGGAGUAC ACAAGACAUACACUACCUUCGCUUCUCCUACAGACUUAACAGAGGGAG AUAGAGAUGGAGGGAGAGCAACCUGGCCAGCGCAAAGAUGCGUAAA	GGGCGAGAGGUUUCAGGACAAACCUUC GCAUACUACUCCUUCUGCACUCC CUCUACUCCACUCUCCACUUAU
27	10	7.4 ± 0.5	GGGUGGUGGAGGAUGGGAAUGGAAGGAGUGGGAGUGUAG AAAGAGAAUACAUACACUACUCCUUCUACUUAACAGAGGGAGA AUAGAAAUGAAGGAGAGCAACCUGGCCAGCGCAAAGAUGCGUAAA	GGGCCUUAAGGGCCUUGGAGGCC GGCAUACACUCACCUUC CAUCAUUCACUCCUCCACCAUAU
28	39	7.4 ± 0.8	GGGAGGAGAAAGAAUAGAAGGUAGAGGGUGGGUGGUAGUUC UAUUAACUGACAAUACACCCGUCUUCUACCUUUAACAGAGGGAGA AUAGAAAUGAAGAAGACGAACCUGGCCAGCGCAAAGAUGCGUAAA	GGGACAUGCGAAGGCCAACUUC UCACGACAUCCACACCGCC UUCUACUUCUCAUUCUCC
29	32	6.6 ± 0.5	GGGAUUGGAGAGAAUAGAAUACAGAGUGAGAUGAGGGAGAGAGUAC UACACAUACCUACUCCUCAUCUACUUC AUACAGAUGGAGAGAGGAACCUGGCCAGCGCAAAGAUGCGUAAA	GGGCCUUAUGGAACGAAGCCA GCAUACUUC UCUGUAAAUCUACUUC CAUUCUCCACCAUAU

Supplementary Table 3. Sequence and performance information for three-way junction (3WJ) repressors

NOTES:

- Trigger RNA sequences are listed up to the base immediately before the T7 terminator used to terminate transcription.
 - Switch RNA sequences are listed up to the 30th base (inclusive) following the end of their trigger binding domain. This 30-nt sequence contains the 21-nt linker sequence and the first 9-nts of GFPmut3b.
 - Devices were measured 3 hr after induction. GFP fluorescence values and their errors are the arithmetic mean and SD, respectively, of n=3 biologically independent samples. Fold reductions for each device are calculated by dividing the GFP fluorescence value from the ON state by the GFP fluorescence value from the OFF state. Relative errors for the fold reductions were obtained by adding the relative fluorescence errors in quadrature.

13	34	34.5 ± 2.2	GGGCAAAGUAUCCAUCAUUUUGUUUAUGUUUAUGAACAGAGGAGACAUACAUGAACAAUCACAUACUAGAACUAAGAACCCUGCGGCAGCGCAAAGAUGCQUAAA	GGGACAUACUACAAUCUAGUAUGUAAUGGAUGGAAUACUUUGAAA	pYZ_3WJrep_N34_switch	ColA/kanamycin	pYZ_3WJrep_N34_trigger	ColE1/ampicillin
14	7	26.2 ± 1.0	GGGCAAAGAUUUAGUAGAUUUUGUUUAUGUUUAUGAACAGAGGAGACAUACAUGAACAAUCGAACGACCAGAACAUAAACCUGCGGCAGCGCAAAGAUGCQUAAA	GGGCGAACGACGAAACGGUCGUUCGGAACUACUAAAUCUUGAAA	pYZ_3WJrep_N07_switch	ColA/kanamycin	pYZ_3WJrep_N07_trigger	ColE1/ampicillin
15	40	23.4 ± 1.8	GGGAUACUUUCAAACUUAUUGUUUAUGUUUAUGAACAGAGGAGACAUACAUGAACAAUCACACUAAUCGACUAAUAAACCUGCGGCAGCGCAAAGAUGCQUAAA	GGGACACUAAUACUACGAUJAGUGUAAUGUUUAGAAG	pYZ_3WJrep_N40_switch	ColA/kanamycin	pYZ_3WJrep_N40_trigger	ColE1/ampicillin
16	11	23.2 ± 3.9	GGGAUCAAUCAUUUCUACUUGUUUAUGUUUAUGAACAGAGGAGACAUACAUGAACAAUCACAUAAACCUAAGAACUAACCUGCGGCAGCGCAAAGAUGCQUAAA	GGGACAUAAACAUAGAGGUJUJAUJAGUAGAAUUGAUUAAG	pYZ_3WJrep_N11_switch	ColA/kanamycin	pYZ_3WJrep_N11_trigger	ColE1/ampicillin
17	33	23.1 ± 0.8	GGGUCCAUUAUCUCAAUUUUGUUUAUGUUUAUGAACAGAGGAGACAUACAUGAACAAUCACCUAAUUCUGAUAUAAACCUGCGGCAGCGCAAAGAUGCQUAAA	GGGAACCUAAUGUACGAAUJAGGUUUAUGUUUAUGUAAG	pYZ_3WJrep_N33_switch	ColA/kanamycin	pYZ_3WJrep_N33_trigger	ColE1/ampicillin
18	9	22.9 ± 5.3	GGGCGAAGAUGAUACAAUJUGUUUAUGUUUAUGAACAGAGGAGACAUACAUGAACAAAGCCACCUACACCUACAUAUAAACCUGCGGCAGCGCAAAGAUGCQUAAA	GGGCACCUCACCUACGUGUGAGGUUCAUUCUUCGUAU	pYZ_3WJrep_N09_switch	ColA/kanamycin	pYZ_3WJrep_N09_trigger	ColE1/ampicillin
19	12	22.9 ± 0.2	GGGUGAUUAGAUAAAGAAUJUGUUUAUGUUUAUGAACAGAGGAGACAUACAUGAACAAAGCCGAUUAUGACUAAUAAACCUGCGGCAGCGCAAAGAUGCQUAAA	GGGCGAUAAUGUUCCGUCAUUAUCGUCAUUCUAAUCAUAG	pYZ_3WJrep_N12_switch	ColA/kanamycin	pYZ_3WJrep_N12_trigger	ColE1/ampicillin
20	36	21.3 ± 0.8	GGGAUGUGAUUACUAGAUUJUGUUUAUGUUUAUGAACAGAGGAGACAUACAUGAACAAUCGAACAGCAAAUCAUACUACAAGAACAUAAACCUGCGGCAGCGCAAAGAUGCQUAAA	GGGCGAACAGAACAUUGCUUGUUCGGAACUAGUAAUCACAUCA	pYZ_3WJrep_N36_switch	ColA/kanamycin	pYZ_3WJrep_N36_trigger	ColE1/ampicillin
21	42	20.8 ± 0.5	GGGAUUCACUUACAAGAUUJUGUUUAUGUUUAUGAACAGAGGAGACAUACAUGAACAAUCACAUAGACCAUAGAACGAACCUGCGGCAGCGCAAAGAUGCQUAAA	GGGACAUAGACAAUJUGGUUCGUJAUJUGUAAUUGAAGUAAUAG	pYZ_3WJrep_N42_switch	ColA/kanamycin	pYZ_3WJrep_N42_trigger	ColE1/ampicillin
22	8	20.5 ± 0.7	GGGACAAACAGAUAAACUUGUUUAUGUUUAUGAACAGAGGAGACAUACAUGAACAAAGCCAAUAGAUAGAACACGAAUACCUUGCGCCAGCGCAAAGAUGCQUAAA	GGGCAAUAGAUCAAACUACUAAUUGCGUUCGUUUAUGUAGC	pYZ_3WJrep_N08_switch	ColA/kanamycin	pYZ_3WJrep_N08_trigger	ColE1/ampicillin
23	1	19.9 ± 2.4	GGGCAAUUAUGUACUAUCCUUGUUUAUGUUUAUGAACAGAGGAGACAUACAUGAACAAAGUCACAUAAACCGCAAACUAAACCUGCGGCAGCGCAAAGAUGCQUAAA	GGGCACAUAAACAUACCGGUUAUGUGACGGAUAGUACAUAAUGAAA	pYZ_3WJrep_N01_switch	ColA/kanamycin	pYZ_3WJrep_N01_trigger	ColE1/ampicillin
24	47	17.5 ± 0.6	GGGCAAUUCCUAACCUUAUUGUUUAUGUUUAUGAACAGAGGAGACAUACAUGAACAAUCAAUAGAGCACAGAACCCUGCGGCAGCGCAAAGAUGCQUAAA	GGGCAAAUAGAUAGAGCUUCUAAUUGGAUAGGUAAUUGAAA	pYZ_3WJrep_N47_switch	ColA/kanamycin	pYZ_3WJrep_N47_trigger	ColE1/ampicillin
25	38	17.0 ± 1.1	GGGAUGAUCGAAACGAAUJUGUUUAUGUUUAUGAACAGAGGAGACAUACAUGAACAAUCACAUAGAACAUAGAACAUAGAACCCUGCGGCAGCGCAAAGAUGCQUAAA	GGGCAAGAAUACAUUCUAAUUCGUUUCGUCAUAAUG	pYZ_3WJrep_N38_switch	ColA/kanamycin	pYZ_3WJrep_N38_trigger	ColE1/ampicillin
26	25	16.1 ± 1.0	GGGUAAGAAUUAAGAAUCAUUGUUUAUGUUUAUGAACAGAGGAGACAUACAUGAACAAUCAGCGAACACCGAAACAUAAACCUGCGCCAGCGCAAAGAUGCQUAAA	GGGAGCGAACAAUACCGGUUCGUUCGUUACGAUUCUAAUAC	pYZ_3WJrep_N25_switch	ColA/kanamycin	pYZ_3WJrep_N25_trigger	ColE1/ampicillin
27	35	15.9 ± 1.0	GGGAUCCAAAGUUUAUCAUUUUGUUUAUGUUUAUGAACAGAGGAGACAUACAUGAACAAUACACAUAAAGACCUCAUAAACCUGCGGCAGCGCAAAGAUGCQUAAA	GGGCACAUAAACUACUUCUUAUGUGUAAUACUUGGUUGAA	pYZ_3WJrep_N35_switch	ColA/kanamycin	pYZ_3WJrep_N35_trigger	ColE1/ampicillin

28	27	15.8 ± 2.1	GGGAAUGAAGAUJAGUGAUUUUGUUAUAGUUAUGAACAGGGAGACAUACAGAACAAUCGAAUAGCGAACUAAGAACCUGGCGGCAGCGAAAAGAUGCGUAAA	GGGCGAAUAAGAAUGCUCUUAUCGGAUACUUAAC	pYZ_3WJrep_N27_switch	ColA/kanamycin	pYZ_3WJrep_N27_trigger	ColE1/ampicillin
29	41	15.4 ± 0.5	GGGAUCUACCGUGUCUAUUGUUAUAGUUAUGAACAGAGGAGACAUACAGAACAAUCACAUCAUCAUAACAGAACCUGGCGGCAGCGCAAAGAUGCGUAAA	GGGAACAUACAAUUGAUGUAUGUUGAUAGACACGGUGAGAUAGA	pYZ_3WJrep_N41_switch	ColA/kanamycin	pYZ_3WJrep_N41_trigger	ColE1/ampicillin
30	45	13.2 ± 0.6	GGGCGACUUAAACAUACUAUUGUUAUAGUUAUGAACAGGGAGACAUACAGAACAAUCACUCCACCGAACUACUAACCUGGCGGCAGCGCAAAGAUGCGUAAA	GGGACUCCACGAUAUCCGUGGAGUUAUGUAGUAG	pYZ_3WJrep_N45_switch	ColA/kanamycin	pYZ_3WJrep_N45_trigger	ColE1/ampicillin
31	4	12.8 ± 1.1	GGGUAAUGAAGUGAAUACUUGUUAUAGUUAUGAACAGGGAGACAUACAGAACAAAGCAAAAGAUACUAAAACCGAACCUUGGCGGCAGCGCAAAGAUGCGUAAA	GGGCAAUAUGAUCAUCGUUAUCUUUGCGCUAUUCACUUAACAA	pYZ_3WJrep_N04_switch	ColA/kanamycin	pYZ_3WJrep_N04_trigger	ColE1/ampicillin
32	48	12.4 ± 1.2	GGGACUACUCCAUUCUAUUGUUAUAGUUAUGAACAGAGGAGACAUACAGAACAAUCGUACAUACUACAAACGAAACCUUGCGCAGCGCAAAGAUGCGUAAA	GGGCAUACCUUACAAUGAGGUAGUAUAGAGGUAG	pYZ_3WJrep_N48_switch	ColA/kanamycin	pYZ_3WJrep_N48_trigger	ColE1/ampicillin
33	37	11.1 ± 0.6	GGGAUGUGAACUAAAAGAUUUGUUAUAGUUAUGAACAGGGAGACAUACAGAACAAUGCGAAAUCGGAAUAGAAACCUUGGCGGCAGCGCAAAGAUGCGUAAA	GGGCGAAAUAACAUACCGUUAUCGGAUUC	pYZ_3WJrep_N37_switch	ColA/kanamycin	pYZ_3WJrep_N37_trigger	ColE1/ampicillin
34	44	10.2 ± 0.3	GGGUACCUUCAAAUCCAUUGUUAUAGUUAUGAACAGGGAGACAUACAGAACAAUCACCUACUAUACAUACUACCUUGGCGGCAGCGCAAAGAUGCGUAAA	GGGACCUACUUACAUUAGUGAGGUAGUGAAUAG	pYZ_3WJrep_N44_switch	ColA/kanamycin	pYZ_3WJrep_N44_trigger	ColE1/ampicillin
35	18	9.6 ± 0.2	GGGCAUCCAUUCAUCAUJGUUAUAGUUAUGAACAGGGAGACAUACAGAACAAUCUCAACAUACUACCUUGGCGGCAGCGCAAAGAUGCGUAAA	GGGCUAACAUACAAUACAGAUUGUUGAGAUGAUGAAUAGGAUUGAGA	pYZ_3WJrep_N18_switch	ColA/kanamycin	pYZ_3WJrep_N18_trigger	ColE1/ampicillin
36	30	9.3 ± 0.7	GGGCGAUJAGAGUAAGAUJGUUAUAGUUAUGAACAGGGAGACAUACAGAACAAUGCAAUAGAACGAUACAAGAACCUUGGCGGCAGCGCAAAGAUGCGUAAA	GGGCAAUAAGAAAACCGUUCUAUUGCAUCUUAUCGUAAU	pYZ_3WJrep_N30_switch	ColA/kanamycin	pYZ_3WJrep_N30_trigger	ColE1/ampicillin
37	22	7.5 ± 0.2	GGGUCAUCCGAUAAUCUUUGUUAUAGUUAUGAACAGGGAGACAUACAGAACAAUJGUACUCAAGGCAAUAGAAACCUUGGCGGCAGCGCAAAGAUGCGUAAA	GGGACUCCAAGAUAGCCUUGGAGUAAAGAUUAUCGUAAU	pYZ_3WJrep_N22_switch	ColA/kanamycin	pYZ_3WJrep_N22_trigger	ColE1/ampicillin
38	6	7.5 ± 0.4	GGGAUUUAGAAGUAAGUAUUGUUAUAGUUAUGAACAGGGAGACAUACAGAACAAUCGAGAACAUAGUGGAACGAAACCUUGGCGGCAGCGCAAAGAUGCGUAAA	GGGCGAAGAUJAGAUACAUACUUCGAAUACUUCUACUAA	pYZ_3WJrep_N06_switch	ColA/kanamycin	pYZ_3WJrep_N06_trigger	ColE1/ampicillin
39	29	7.5 ± 0.3	GGGACUCCAUUUGACGAUJGUUAUAGUUAUGAACAGGGAGACAUACAGAACAAUACAUAAUAGACUAAACAUAAACCUUGGCGGCAGCGCAAAGAUGCGUAAA	GGGCAUAUAGAAUAGAGGUUAUAGUAGUAGA	pYZ_3WJrep_N29_switch	ColA/kanamycin	pYZ_3WJrep_N29_trigger	ColE1/ampicillin
40	31	7.0 ± 0.4	GGGAAUGAUGAUGAGAUUUGUUAUAGUUAUGAACAGGGAGACAUACAGAACAAUAGACGGAACGAGCAAUGGAAACCUUGGCGGCAGCGCAAAGAUGCGUAAA	GGGAGCGAACCGCGAACUCGUUCGCUAAUCUACUUAAG	pYZ_3WJrep_N31_switch	ColA/kanamycin	pYZ_3WJrep_N31_trigger	ColE1/ampicillin
41	39	6.1 ± 0.1	GGGCGAAUJUGAAAUGAAUUGUUAUAGUUAUGAACAGGGAGACAUACAGAACAAUAGACGGAACGAGCAAACCUUGGCGGCAGCGCAAAGAUGCGUAAA	GGGACGGAAUACACUCUUAUCCGUCAUUCAUUCGUAA	pYZ_3WJrep_N39_switch	ColA/kanamycin	pYZ_3WJrep_N39_trigger	ColE1/ampicillin

42	26	5.6 ± 0.6	GGGUUUACUUACCGAUUUGUUUAUGUUAUGAACAGGGAGACAUACAUGAACAAUCUCCAACGGAACAUCAACCUGGCGGCAGCGCAAAGAUGC GUAAA	GGGACUCCAACUAACCGUUGGAGU GAUAUCGGUAAGUUAUGAA	pYZ_3WJrep_N26_switch	ColA/kanamycin	pYZ_3WJrep_N26_trigger	ColE1/ampicillin
43	43	5.2 ± 0.4	GGGCAUUUACCUUACUAUUUGUUUAUGUUAUGAACAGGGAGACAUACAUGAACAAUACACUCCAACAUCAAAGUAACCUGGCGGCAGCGCAAAGAUGC GUAAA	GGGCACUCCAAUAGGAUUGGAGUG UAAUAGUAGGUAAAUGAGA	pYZ_3WJrep_N43_switch	ColA/kanamycin	pYZ_3WJrep_N43_trigger	ColE1/ampicillin
44	28	4.6 ± 0.1	GGGAUUUACUUAGAUACUUUGUUUAUGUUAUGAACAGGGAGACAUACAUGAACAAUUAACAUUAACAUACG AACGAACCUGGCGGCAGCGCAAAGAUGC GUAAA	GGGACAUAUACUUUCAUGUAU AUGUAAGUAUCUAGUAAAUGAA	pYZ_3WJrep_N28_switch	ColA/kanamycin	pYZ_3WJrep_N28_trigger	ColE1/ampicillin
45	46	4.0 ± 0.0	GGGCUCAUACUUCACAUUUUGUUUAUGUUAUGAACAGGGAGACAUACAUGAACAAUACACCACAUAAU CACUAACCUGGCGGCAGCGCAAAGAUGC GUAAA	GGGCACCUAACUAACAUUGGUAGGUG UAAUAGUGAAGUAUGAGAUG	pYZ_3WJrep_N46_switch	ColA/kanamycin	pYZ_3WJrep_N46_trigger	ColE1/ampicillin
46	5	2.9 ± 0.1	GGGAUCUCCAUCUAUCCAUUUGUUUAUGUUAUGAACAGGGAGACAUACAUGAACAAUCCAUUAAGUAAACAGCAGAACCUUGGCGGCAGCGCAAAGAUGC GUAAA	GGGCAUUAAGUUAGUUACUUUAUG GAUGGAUAGAUGGAGAUGAU	pYZ_3WJrep_N05_switch	ColA/kanamycin	pYZ_3WJrep_N05_trigger	ColE1/ampicillin
47	14	2.2 ± 0.0	GGGUAGAUUAAGAGUGAUUUGUUUAUGUUAUGAACAGGGAGACAUACAUGAACAAUGACCUAACGCACG AACUAACCUGGCGGCAGCGCAAAGAUGC GUAAA	GGGACCUAACUAACGCGUUUAGGU CAAUCACUCUUAAUCUACUA	pYZ_3WJrep_N14_switch	ColA/kanamycin	pYZ_3WJrep_N14_trigger	ColE1/ampicillin
48	17	2.0 ± 0.1	GGGCAAUUCCAAUACGUUUGUUUAUGUUAUGAACAGGGAGACAUACAUGAACAGCACUAAAACCGAAU ACUAACCUGGCGGCAGCGCAAAGAUGC GUAAA	GGGACUUAACGAAACGGUUUAAGU GCACGUUUGGAGAUUGGGA	pYZ_3WJrep_N17_switch	ColA/kanamycin	pYZ_3WJrep_N17_trigger	ColE1/ampicillin

Supplementary Table 4. Sequence information for repressors with inducible promoters

NOTES:

1. Trigger RNA sequences are listed up to the base immediately before the terminator.

2. Switch RNA sequences are listed from RiboJ up to the 30th base (inclusive) following the end of their trigger binding domain. This 30-nt sequence contains the 21-nt linker sequence and the first 9-nts of GFPmut3b.

First generation toehold repressor index	Switch sequence	Switch promoter	Switch terminator	Trigger sequence	Trigger promoter	Trigger terminator	Switch plasmid	Switch plasmid origin/Resistance	Trigger plasmid	Trigger plasmid origin/Resistance
1	AGCUGUCACCGGAUGUGCUUCCGGUCUG AUGAGUCCGUGAGGACGAAACAGCCUCUAC AAAUAAAUUUUGUUAAAAGAAAGAUAA GAUAGUGUGAUGAAGUGCGAAGUUGUAU AACAAAUUACUAUUACUACUUUCGCUUCA UCUCAUCUAUAAACAGAGGGAGAAUAGAUU GAUGAAGAGCAACCUGCGGCAGCGCAAAA GAUGCUGAAA	Ptet*	terminator_1	GGGUUCAGACAAACCGGUAGGUUU GUCUGAAUUAUUAUACACUUCGCA CUUCAUCACAUCAUCUUAUCU CAUUUCUAAAC	PluxB	T7 terminator	pAG_Ptet*_ToeRep_N01_switch	ColA/kanamycin	pAG_PluxB_ToeRep_N01_trigger	CDF/spectinomycin
19	AGCUGUCACCGGAUGUGCUUCCGGUCUG AUGAGUCCGUGAGGACGAAACAGCCUCUAC AAAUAAAUUUUGUUAAAACUAUACAGAUCA CUUGUUUAUGUUAUGAACAGAGGGAGACAU ACAUGAACAAAGCACCUAACAGACUAUCA ACCUGGGCGCAGCGAAAGAUGCUGAAA	Ptet*	terminator_1	GGGACCUAACAUAAACUUGUUAGG UGCGUAGAUCUGAUUAGUGUG	PluxB	terminator_2	pYZ_Ptet*_3WJrep_N19_switch	ColA/kanamycin	pYZ_PluxB_3WJrep_N19_trigger	ColE1/ampicillin

Supplementary Table 5. Sequence and performance information for 3WJ repressors with altered stems

NOTES:

1. Trigger RNA sequences are listed up to the base immediately before the T7 terminator used to terminate transcription.
2. Switch RNA sequences are listed up to the 30th base (inclusive) following the end of their trigger binding domain. This 30-nt sequence contains the 21-nt linker sequence and the first 9-nts of GFPmut3b.
3. Devices were measured 3 hr after induction. GFP fluorescence values and their errors are the arithmetic mean and SD, respectively, of n=3 biologically independent samples. Fold reductions for each device are calculated by dividing the GFP fluorescence value from the ON state by the GFP fluorescence value from the OFF state. Relative errors for the fold reductions were obtained by adding the relative fluorescence errors in quadrature.

GFP fold reduction	Switch sequence	Trigger sequence	Switch plasmid	Switch plasmid origin/Resistance	Trigger plasmid	Trigger plasmid origin/Resistance
42.1 ± 3.4	GGGAAAGUGAAGAAGAAUUAAG UGAAUGAAGGCGAUGAUUGUAAG GUUACUACACUUACACUCAUCGCU UUCAUCUACUUUAACAGAGG AGAAUAAAAGAUGAAUGAAGCAACC UGGCAGCGCAGCGCAAAGAUGC AA	GGGUCAAGGCAUUAGCCUAAU GCCUUGAAUACUUACAAUCAUCG CCUUCAUCAACUUUAUUCU UCUUCACUUUACU	pYZ_3WJrep_N20_switch	ColA/kanamycin	pYZ_3WJrep_N20_trigger	ColE1/ampicillin
1.1 ± 0.4	GGGAUGAAUGAUUAACACGGUUGA GGCAGUGGAACAGAGGGAGACCACU GAUGCAACCAGCACGAAUUGACUAC ACUAACCUGGCAGCGCAA GAUGCG AAA	GGGUCAAGGCAUUAGCCUAAU GCCUUGAAUACUUACAAUCAUCG CCUUCAUCAACUUUAUUCU UCUUCACUUUACU	pYZ_3WJrep_N20_switch_NNvA	ColA/kanamycin	pYZ_3WJrep_N20_trigger	ColE1/ampicillin
1.0 ± 0.1	GGGAUGAAUGAUUAACACGGUAAA GGCUAUCGAACAGAGGGAGACGAUA GAUGUUACCGCACGAAUUGACUAC ACUAACCUGGCAGCGCAA GAUGCG AAA	GGGUCAAGGCAUUAGCCUAAU GCCUUGAAUACUUACAAUCAUCG CCUUCAUCAACUUUAUUCU UCUUCACUUUACU	pYZ_3WJrep_N20_switch_NNvB	ColA/kanamycin	pYZ_3WJrep_N20_trigger	ColE1/ampicillin
1.0 ± 0.1	GGGAUGAAUGAUUAACACUUGAUA GGCUAUUGAACAGAGGGAGACAAUA GAUGAUCAAGCACGAAUUGACUAC ACUAACCUGGCAGCGCAA GAUGCG AAA	GGGUCAAGGCAUUAGCCUAAU GCCUUGAAUACUUACAAUCAUCG CCUUCAUCAACUUUAUUCU UCUUCACUUUACU	pYZ_3WJrep_N20_switch_SWvA	ColA/kanamycin	pYZ_3WJrep_N20_trigger	ColE1/ampicillin
41.2 ± 5.1	GGGAUGAAUGAUUAACACAUGUAA ACCUAUUGAACAGAGGGAGACAAUA GAUGUACAUAGCACGAAUUGACUAC ACUAACCUGGCAGCGCAA GAUGCG AAA	GGGUCAAGGCAUUAGCCUAAU GCCUUGAAUACUUACAAUCAUCG CCUUCAUCAACUUUAUUCU UCUUCACUUUACU	pYZ_3WJrep_N20_switch_SWvB	ColA/kanamycin	pYZ_3WJrep_N20_trigger	ColE1/ampicillin
32.6 ± 5.0	GGGAUGAAUGAUUAACACUUGAUA AGCUUAUGAACAGAGGGAGACAAUA GAUGAUCAAGCACGAAUUGACUAC ACUAACCUGGCAGCGCAA GAUGCG AAA	GGGUCAAGGCAUUAGCCUAAU GCCUUGAAUACUUACAAUCAUCG CCUUCAUCAACUUUAUUCU UCUUCACUUUACU	pYZ_3WJrep_N20_switch_SWvC	ColA/kanamycin	pYZ_3WJrep_N20_trigger	ColE1/ampicillin

Supplementary Table 6. Sequence and performance information for second-generation toehold repressors

NOTES:

- Trigger RNA sequences are listed up to the base immediately before the T7 terminator used to terminate transcription.
 - Switch RNA sequences are listed up to the 30th base (inclusive) following the end of their trigger binding domain. This 30-nt sequence contains the 21-nt linker sequence and the first 9-nts of GFPmut3b.
 - Devices were measured 3 hr after induction. GFP fluorescence values and their errors are the arithmetic mean and SD, respectively, of n=3 biologically independent samples. Fold reductions for each device are calculated by dividing the GFP fluorescence value from the ON state by the GFP fluorescence value from the OFF state. Relative errors for the fold reductions were obtained by adding the relative fluorescence errors in quadrature.

15	17	59.9 ± 2.2	GGGAAAGAUGAAAUGAAGAUGAAGGGGAAGUJGGAGUGUGUAGA UUACGAAACUUAACACACCUCCACUCCACCUUCAAUAACAGAGGAG AAUAGAAAUGGAAGUAGGAACCUGGGCGACGCACAAAGAUGC GGGCUAUUCAACCAACACGAUGGUGUAAG ACGACUUAACACACACCUCCACUCCAC UUCUCAUUCUCAUUCAUCUUACU pJK_ToeRepG2_N17_switch	ColA/kanamycin	pJK_ToeRepG2_N17_trigger	CDF/spectinomycin
16	46	58.9 ± 3.1	GGGAGAGAAGAAGAAGAAGAACCGGAAUAGUGCGAAAGUAGAAA UAAUCAUAAUUCUACUUCGCCUCAUUCUUCGUUCAAUAACAGAGGAG AUAGAAAUGGAAGAGCAACCUGGGCGACGCACAAAGAUGC GGGUCAGAUGUGAUGGCCUCACAU GAAACAUUUCAUCUUCUUCGACUUAUC CGUUCUACUUCUCAUCUUCU pJK_ToeRepG2_N46_switch	ColA/kanamycin	pJK_ToeRepG2_N46_trigger	CDF/spectinomycin
17	56	47.4 ± 3.3	GGGAUGGAGAAGAAGAUGAUAUGAAGGAGAUGGGGUUJGGAGU CAACACAUACACUCAACCCUCAUCUUCUUCUCAAUAACAGAGGAG AAUJGAAAUGGAJUGGAGAACCCUGGGCGACGCACAAAGAUGC GGGCGUACUUCGACCUGGGCAAGU CGCAGAACUCAACUCCACUUC CUCUCAUACUUCUUCU pJK_ToeRepG2_N56_switch	ColA/kanamycin	pJK_ToeRepG2_N56_trigger	CDF/spectinomycin
18	21	47.0 ± 2.1	GGGAUGGAGAAGAAGAUGAUAUGAAGAGGCAGAUGAUGUAGU CAACUUCUACUACAAUACUGUCUJCACUUCUCAAUAACAGAGGAG AAUAGAAAUGGAAGAGAGCAACCCUGGGCGACGCACAAAGAUGC GGGUCACUACACACAU GAAUACACUACACAU CUUCUCAUCUCAUCU pJK_ToeRepG2_N21_switch	ColA/kanamycin	pJK_ToeRepG2_N21_trigger	CDF/spectinomycin
19	75	44.8 ± 3.8	GGGAUGGAGAAGAAGAUAAGGGUGAAGAUGCGUJUGGUAGU AUAAUCGAAACAUACACACGUCAUCUCAUCUCAAUAACAGAGGAG AUAGAAAUGGAAGAGCAACCUGGGCGACGCACAAAGAUGC GGGAGUCCCUGGUUUAUACACAGGGA CUCUAAACUACACAGCCACU CUUCUAAUUCUCAUCU pJK_ToeRepG2_N75_switch	ColA/kanamycin	pJK_ToeRepG2_N75_trigger	CDF/spectinomycin
20	44	43.0 ± 5.3	GGGAAQUAAGAAGUGAAAAGAAGAAGAGGCAGAGUGUAGU CAAUUCUAAUJACAUACUUCGCUUUCUACUUCUUAACAGAGGAG AUAAAGAUGGAAGAGCAACCUGGGCGACGCACAAAGAUGC GGGUCAGUUCUACUAGCAUCUAGGAAC GAAUAAUACACACUUC UUUCUUAUUCACUUC pJK_ToeRepG2_N44_switch	ColA/kanamycin	pJK_ToeRepG2_N44_trigger	CDF/spectinomycin
21	88	42.2 ± 4.9	GGGAAUGGAGAAGAAGGAGAUAAGGGGGAAAGUGGGAGUG ACUUCUAAUCUUCUACACCCUCAUUCGACCUUAAAACAGAGGAG AUAAAGAUGGAAGAGGAACCUGGGCGACGCACAAAGAUGC GGGCGAGCCGCCU GCAACUUCUACACU CACCUUAAUCC pJK_ToeRepG2_N88_switch	ColA/kanamycin	pJK_ToeRepG2_N88_trigger	CDF/spectinomycin
22	77	40.6 ± 2.7	GGGAGAGAUGUGAAGAUGUAGAAAUGGAAGAGCGAAGU AAAUAACAAUACACACUUCGCUUCUCAUCUCAAUAACAGAGGAG AUAGAAAUGGAAGAGCAACCCUGGGCGACGCACAAAGAUGC GGGACGAGGCC GUCAUACAAAC UUUCAUC pJK_ToeRepG2_N77_switch	ColA/kanamycin	pJK_ToeRepG2_N77_trigger	CDF/spectinomycin
23	52	40.3 ± 2.8	GGGAUGGAGAAGAUAUAGGGUGAGAGUGGGUUGAGU UUACUUAACACACUACCUACUCACGCCUCAUAAACAGAGGAG AAUAGAGAUGGGAGAGUAGGAACCUGGGCGACGCACAAAGAUGC GGGCGUAGAGGU GCAACAA CUCUAC CUCU pJK_ToeRepG2_N52_switch	ColA/kanamycin	pJK_ToeRepG2_N52_trigger	CDF/spectinomycin
24	43	39.3 ± 1.9	GGGAGAGAAGAUAAGAAGAAAAGAGGGAAUGAGGUGUG AACUUCUACUAAACACACCUCAUCCAUUCUAAAACAGAGGAG AUAAAGAUGGGAAUGAGGAACCUGGGCGACGCACAAAGAUGC GGGCGACU GCAACUAC UCC pJK_ToeRepG2_N43_switch	ColA/kanamycin	pJK_ToeRepG2_N43_trigger	CDF/spectinomycin
25	8	37.6 ± 4.1	GGGAGAGAAAAAGAGAAAAGAUAGGAGGAAGUGGGAG CUCAAAUUCUUCUACUCUCCACUUCUCAUCUAAAACAGAGGAG AUAGAAUGGGAGUGGAACCUGGGCGACGCACAAAGAUGC GGGCUUAC GCA UAC pJK_ToeRepG2_N08_switch	ColA/kanamycin	pJK_ToeRepG2_N08_trigger	CDF/spectinomycin
26	3	36.1 ± 12.3	GGGAGAAUUAUGAAAUGGAGUGAAGGGAGUGAGGUJUGA UAUUCAGCACA AUAGAAAUGG GGGCGACCG pJK_ToeRepG2_N03_switch	ColA/kanamycin	pJK_ToeRepG2_N03_trigger	CDF/spectinomycin
27	89	34.5 ± 1.6	GGGAGAGAUAUGGAGAAAAGAAGAAGGGAGGAUGUGAG UCAUACACU AUAGAAAUG GGGCGU pJK_ToeRepG2_N89_switch	ColA/kanamycin	pJK_ToeRepG2_N89_trigger	CDF/spectinomycin
28	42	34.1 ± 10.6	GGGGUAAAAGAGUGUGUGAAAGAGGUAGAGGAGCG ACAUAGAU AUAGAAAUG GGGCUU pJK_ToeRepG2_N42_switch	ColA/kanamycin	pJK_ToeRepG2_N42_trigger	CDF/spectinomycin
29	15	34.1 ± 2.3	GGGAAGAAAGUAAAUGGAGAUGAAGAGGAGAUAGAGGAG UUAAUAAUC AUAGAAAUG GGGCGC pJK_ToeRepG2_N15_switch	ColA/kanamycin	pJK_ToeRepG2_N15_trigger	CDF/spectinomycin
30	86	33.9 ± 1.9	GGGGUAAAAGAGUGAAGAGGAGGAUGUGUG ACUUAAC AUAGAAAUG GGGCGG pJK_ToeRepG2_N86_switch	ColA/kanamycin	pJK_ToeRepG2_N86_trigger	CDF/spectinomycin
31	1	33.2 ± 1.4	GGGAAGAUAAAUGGAGAUGAAGAGGAGUGAUG GGACGAG AUAGAAAUG GGGAG pJK_ToeRepG2_N01_switch	ColA/kanamycin	pJK_ToeRepG2_N01_trigger	CDF/spectinomycin

66	7	13.9 ± 2.0	GGGAAAGUAAAUGAGUGAUAAGAUAGAAGUGCGGAUGUGUGUUAGAU UCAACAUUCUACACACAUCCGACUUCAUCUUAACAGAGGG AAUAGAAAUGAGAACGUAGCACCUGCGGCAGCGAAAGAUGC GGGACCUAUGCACUACCGCAUAGG GUAAACUAACACACAUCCGACUUCAU CUUCUACAUCAUUACUU pJK_ToeRepG2_N07_switch	ColA/kanamycin	pJK_ToeRepG2_N07_trigger	CDF/spectinomycin
67	54	13.9 ± 1.4	GGGGUAAGAGAAUGUGUGAUAAGAGGAUGAGAAGGGAU CUCGAAAUACACAAACAUCCAUUCU AAUAGAAAUGAGAGAACGUAGCACC GGGUUCUGGUCAUCAACAUCAUGA GACUAAUACACACAA CUCUUAUCACU pJK_ToeRepG2_N54_switch	ColA/kanamycin	pJK_ToeRepG2_N54_trigger	CDF/spectinomycin
68	32	13.6 ± 1.6	GGGAAAGAGAGUGGGAAUAGAGGUAGAGGAAGGGCUU CACAGAACACAUCAAGC AAUAGAGAUGGGAGGAAGC GGGCCAAGCA GGGCCAAGCA pJK_ToeRepG2_N32_switch	ColA/kanamycin	pJK_ToeRepG2_N32_trigger	CDF/spectinomycin
69	67	13.5 ± 3.8	GGGAGAAGUAAAUGAGUGAUAAGUAGAGAAC CAGAAAACA AUAGAU GGGCGAGAGA GGGUCC pJK_ToeRepG2_N67_switch	ColA/kanamycin	pJK_ToeRepG2_N67_trigger	CDF/spectinomycin
70	47	13.5 ± 1.3	GGGAAAGUAAAUGAGAUAGAAGUAGAGAAC AACAAU AAUAGAGAAG GGGU GGGU pJK_ToeRepG2_N47_switch	ColA/kanamycin	pJK_ToeRepG2_N47_trigger	CDF/spectinomycin
71	28	12.7 ± 1.6	GGGAAAUAAUAGGGAGAGAUAAGAGGG CUUACCU AUAGAGA GGGCG GGGCG pJK_ToeRepG2_N28_switch	ColA/kanamycin	pJK_ToeRepG2_N28_trigger	CDF/spectinomycin
72	9	12.4 ± 1.6	GGGAAAGUAAAAGAGAGUAUAAGAGAG UGACG AAUAGAGA GGGU GGGU pJK_ToeRepG2_N09_switch	ColA/kanamycin	pJK_ToeRepG2_N09_trigger	CDF/spectinomycin
73	29	12.3 ± 4.5	GGGAAAGUAGAGAGAAUAAA CGGC AUUAAA GGGU GGGU pJK_ToeRepG2_N29_switch	ColA/kanamycin	pJK_ToeRepG2_N29_trigger	CDF/spectinomycin
74	80	12.1 ± 0.6	GGGAGAGAUGAUGGAAGAAA AGAAA AAUAAA GGGU GGGU pJK_ToeRepG2_N80_switch	ColA/kanamycin	pJK_ToeRepG2_N80_trigger	CDF/spectinomycin
75	13	11.7 ± 2.2	GGGAUGAGAAA AGCCG AUAAA GGGU GGGU pJK_ToeRepG2_N13_switch	ColA/kanamycin	pJK_ToeRepG2_N13_trigger	CDF/spectinomycin
76	23	11.7 ± 0.8	GGGAAUGAAA CUU AUAAA GGGU GGGU pJK_ToeRepG2_N23_switch	ColA/kanamycin	pJK_ToeRepG2_N23_trigger	CDF/spectinomycin
77	12	11.6 ± 3.3	GGGAAAGUAGUAAA ACAA AAUAGAG GGGU GGGU pJK_ToeRepG2_N12_switch	ColA/kanamycin	pJK_ToeRepG2_N12_trigger	CDF/spectinomycin
78	10	11.1 ± 1.9	GGGAGAGUAGAG UCU AAUAGAG GGGU GGGU pJK_ToeRepG2_N10_switch	ColA/kanamycin	pJK_ToeRepG2_N10_trigger	CDF/spectinomycin
79	5	10.9 ± 1.0	GGGAAAGUAAAAGAGAG CAAA AUAAA GGGU GGGU pJK_ToeRepG2_N05_switch	ColA/kanamycin	pJK_ToeRepG2_N05_trigger	CDF/spectinomycin
80	60	10.7 ± 1.2	GGGAGAAA AAC AAUAGAG GGGU GGGU pJK_ToeRepG2_N60_switch	ColA/kanamycin	pJK_ToeRepG2_N60_trigger	CDF/spectinomycin
81	74	10.6 ± 0.9	GGGAGAGAAG UCA AAUAGAG GGGU GGGU pJK_ToeRepG2_N74_switch	ColA/kanamycin	pJK_ToeRepG2_N74_trigger	CDF/spectinomycin
82	69	9.9 ± 1.8	GGGAGAGUAGAGAG GUU AAUAGAG GGGU GGGU pJK_ToeRepG2_N69_switch	ColA/kanamycin	pJK_ToeRepG2_N69_trigger	CDF/spectinomycin

Supplementary Table 7. Shortened Triggers for SHAPE-Seq Study of 3WJ Repressors 21 and 13

NOTE:

Trigger RNA sequences include the T7 terminator sequence

Trigger name	Shortened 3WJ Repressor Trigger Sequence	Plasmid Name
Trig7_len18	GGGUGCUCGCGUUAGAGCACCCAGUGUCGGAUAAAGUGAAUUAUAGCAUAACCCCUUGGGGCCUCUAAACGGGUUCUUGAGGGGUUUUUUG	pYZ_3WJrep_N21_triggerA18
Trig7_len20	GGGUGCUCGCGUUAGAGCACCCUAGUGUCGGAUAAAGUGAAUUAUAGCAUAACCCCUUGGGGCCUCUAAACGGGUUCUUGAGGGGUUUUUUG	pYZ_3WJrep_N21_triggerA20
Trig7_len25	GGGUGCUCGCGUUAGAGCACCCGUAGUGUCGGAUAAAGUGAAUAGUAGCAUAACCCCUUGGGGCCUCUAAACGGGUUCUUGAGGGGUUUUUUG	pYZ_3WJrep_N21_triggerA25
Trig8_len18	GGGCCUGCGGCAGAGCAGGCCUUGUAUGUGAUUUUAGCAUAACCCCUUGGGGCCUCUAAACGGGUUCUUGAGGGGUUUUUUG	pYZ_3WJrep_N13_triggerA18
Trig8_len20	GGGUGCUCGCGUUAGAGCACCCUUGUAUGUGAUUUUAGCAUAACCCCUUGGGGCCUCUAAACGGGUUCUUGAGGGGUUUUUUG	pYZ_3WJrep_N13_triggerA20

Supplementary Table 8. Indices for Orthogonal Sets of Toehold and 3WJ Repressors

A. Sets of orthogonal toehold repressors with different crosstalk levels

Toehold Repressor Libraries Selected After 3-hr Induction

Library Size	Toehold Repressor Indices	Library Dynamic Range (3 hr)
14	3,4,16,30,36,41,42,49,65,76,78,86,91,95	1.5
13	3,4,16,30,36,41,42,49,65,78,86,91,95	1.6
12	3,4,16,30,36,42,49,59,65,78,91,95	1.7
11	3,16,30,36,41,42,49,65,76,78,86	2.5
10	3,16,30,36,41,42,65,76,78,86	2.8
9	3,4,16,30,36,49,86,91,95	4.9
8	16,30,36,42,76,78,86,91	7.0
7	16,30,42,78,86,91,95	7.3
6	3,16,36,49,78,86	7.5
5	16,30,49,78,86	8.7
4	16,30,78,86	12.0
3	30,36,78	15.8
2	59,77	24.4

B. Sets of orthogonal 3WJ repressors with different crosstalk levels

3WJ Repressor Libraries Selected After 3-hr Induction

Library Size	3WJ Repressor Indices	Library Dynamic Range (3 hr)	Library Dynamic Range (4 hr)	Library Dynamic Range (5 hr)
16	2,3,7,10,11,12,13,15,19,20,21,23,24,32,34,40	3.1	6.5	11.6
15	2,3,7,10,11,12,13,15,20,21,23,24,32,34,40	18.2	24.9	23.9
14	2,3,7,10,11,13,15,20,21,23,24,32,34,40	18.5	24.9	23.9
13	2,3,7,10,11,13,15,20,21,23,24,32,34	20.1	24.9	23.9
12	2,3,10,11,13,15,20,21,23,24,32,34	23.9	28.6	23.9
11	2,3,10,11,13,15,20,21,24,32,34	24.2	28.6	23.9
10	2,3,10,13,20,21,23,24,32,34	25.6	28.6	23.9
9	2,3,10,13,20,21,23,24,32	28.4	28.6	23.9
8	2,3,10,13,20,21,23,32	29.2	57.4	42.1
7	3,10,13,20,23,24,32	30.8	48.0	41.3
6	10,20,21,23,24,32	40.0	47.4	42.1
5	10,20,23,24,32	43.5	51.1	42.1
4	19,20,21,32	47.7	62.6	50.6
3	19,20,32	63.8	118.7	100.6
2	20,32	87.1	145.0	122.5

3WJ Repressor Libraries Selected After 4-hr Induction

Library Size	3WJ Repressor Indices	Library Dynamic Range (3 hr)	Library Dynamic Range (4 hr)	Library Dynamic Range (5 hr)
16	2,3,7,10,11,12,13,15,19,20,21,23,24,32,34,40	3.1	6.5	11.6
15	2,3,7,10,11,12,13,15,20,21,23,24,32,34,40	18.2	24.9	23.9
14	2,3,10,11,12,13,15,20,21,23,24,32,34,40	18.2	28.6	23.9
13	3,10,11,12,13,15,20,21,23,24,32,34,40	18.2	32.7	32.9
12	3,10,11,13,15,20,21,23,24,32,34,40	18.5	39.3	32.9
11	2,3,10,13,15,20,21,23,32,34,40	18.5	40.0	42.1
10	2,3,10,13,15,20,21,23,32,40	18.5	41.7	42.1
9	2,3,10,13,15,20,21,23,32	23.9	50.9	42.1
8	2,3,10,13,20,21,23,32	29.2	57.4	42.1
7	2,3,10,13,20,21,32	29.2	61.3	50.6
6	2,3,10,13,20,32	33.6	70.3	66.7
5	3,10,13,20,32	36.2	75.8	66.7
4	10,13,20,32	40.0	90.2	66.7
3	2,20,21	42.4	126.5	131.0
2	2,20	67.8	197.5	237.2

3WJ Repressor Libraries Selected After 5-hr Induction

Library Size	3WJ Repressor Indices	Library Dynamic Range (3 hr)	Library Dynamic Range (4 hr)	Library Dynamic Range (5 hr)
16	2,3,7,10,11,12,13,15,19,20,21,23,24,32,34,40	3.1	6.5	11.6
15	2,3,7,10,11,12,13,15,19,20,21,23,24,32,34	14.0	23.9	23.9
14	2,3,7,10,11,12,13,15,19,20,21,23,32,34	14.0	23.9	38.0
13	2,3,10,11,12,13,15,20,21,23,32,34,40	18.2	32.7	42.1
12	2,3,10,11,12,13,15,19,20,21,23,34	14.0	32.7	55.1
11	2,3,10,11,12,13,15,20,21,34,40	18.4	34.4	61.1
10	2,3,10,12,13,15,19,20,21,34	14.0	33.3	64.3
9	2,3,10,12,13,15,20,21,40	18.4	34.4	69.0
8	2,3,10,13,15,20,21,40	18.5	41.7	72.7
7	2,3,10,13,15,20,21	24.3	52.3	86.2
6	2,10,13,15,20,21	24.3	52.3	118.4
5	2,10,13,15,20	27.0	63.6	145.9
4	2,10,13,20	33.6	75.1	164.6
3	10,13,20	40.0	90.2	196.6
2	2,20	67.8	197.5	237.2

Supplementary Table 9. mRNA Sensors and Trigger Sequences

A. Toehold Repressor mRNA Sensors

mRNA Sensor	Sensor Sequence	mRNA Target Subsequence	Full mRNA Target Sequence
kanR sensor	GGGUUAUUCAUACAGGAUUAUCAAUACCAUAUUUUUGAAAAA GCCGUUUCGUUAUGAAGGACUCCACAUACCUUCGUUACAGA UACGGCUUGUICAAAAAACAGAGGAGAUUJUGAUGGCCU AUCAACCUUGGCCGCGCACAAGAUGGUAAA	UCCUCAUUAACAGAAACGCCUUUUUCAA AUGGUUUGUAUACCUGAUUAGAAUA	AUGAGCCAUUUCAACGGGAACGUUCUUCAGGCCGAUJAAU UCUACGCAUJGUAGGGAAGCCGAUAGGCCAGAGUUGU UGCCCUUCGCCACAUACGCAUJUUUACCGUACUCC AAUAAUUAUGUAGGCCUUCGCCGCUU AAUACCGGUU CAUGGUJAUU UGCCUCCGG GAAACU GGGGAAACAGGAAGGAAAUAGCGCAAAAGGGGAUAGGGG ACACGGAAAUUGUCAAUACAAUACAGUJAUUCUACAUJUCC GUGUCGACAUUACAAACAGAGGAGAGAUAAAUGCGACACG GAAACUCCGGGGCAGGCCAAAGAUGGUAAA
bla sensor		GUUUUCAACAUUUCGGUGUCCCUU GUUUUUGCCGUU GGGGAAACAGGAAGGAAAUAGCGCAAAAGGGGAUAGGGG ACACGGAAAUUGUCAAUACAAUACAGUJAUUCUACAUJUCC GUGUCGACAUUACAAACAGAGGAGAGAUAAAUGCGACACG GAAACUCCGGGGCAGGCCAAAGAUGGUAAA	AUGAGGUUUCAACAUUCCGGUGUCCCUU UGACAGGUU GUUUUUGCCGUU GGGGAAACAGGAAGGAAAUAGCGCAAAAGGGGAUAGGGG ACACGGAAAUUGUCAAUACAAUACAGUJAUUCUACAUJUCC GUGUCGACAUUACAAACAGAGGAGAGAUAAAUGCGACACG GAAACUCCGGGGCAGGCCAAAGAUGGUAAA

B. 3WJ Repressor mRNA Sensors

mRNA Sensor	Sensor Sequence	mRNA Target Subsequence	Full mRNA Target Sequence
KanR sensor	GGGAGGACAAUUCACAAUUCGUUUAUAGUUAUGAACAGAGGAGA CAUAAACAUAGAACAGGAUCAUAGAAUAGAACCUUGGCC AGCGCAAAAGAUGGUAAA	CAUUCGAUUCGUU GGGGAGGACAAUUCACAAUUCGUUUAUAGUUAUGAACAGAGGAGA CAUAAACAUAGAACAGGAUCAUAGAAUAGAACCUUGGCC AGCGCAAAAGAUGGUAAA	AUGAGCCAUUUCAACGGGAACGUUCUUCAGGCCGAU UCUACGCAUJGUAGGGAAGCCGAUACAGGGGAAG UGCCCUUCGCCACAUACGCAUJUUUACCGUACUCC AAUAAUUGUUGAUGGCCUUCGCCG AAUACCGGUU AAUACCGGUU CAUGGUJAUU UGCCUCCGG GGGGAGGACAAUUCACAAUUCGUUUAUAGUUAUGAACAGAGGAGA CAUAAACAUAGAACAGGAUCAUAGAAUAGAACCUUGGCC AGCGCAAAAGAUGGUAAA
aadA sensor	GGGUUAGGCCUCAAAAUUUGUUAUAGUUAUGAACAGAGGAGA CAUAAACAUAGAACAGGAUCCUGUUCAGCACAUACCUUGGCC AGCGCAAAAGAUGGUAAA	CUGAACAGGAUCU GGGGAGGACAAUUCACAAUUCGUUUAUAGUUAUGAACAGAGGAGA CAUAAACAUAGAACAGGAUCCUGUUCAGCACAUACCUUGGCC AGCGCAAAAGAUGGUAAA	AUGAGGGAAGCGUGAUCGCCGAAGUAUCACAUAC GAGAGCGAGAU GGGGAGGACAAUUCACAAUUCGUUUAUAGUUAUGAACAGAGGAGA CAUAAACAUAGAACAGGAUCCUGUUCAGCACAUACCUUGGCC AGCGCAAAAGAUGGUAAA

Supplementary Table 10. NAND Gate and NOR Gate Circuit RNA Sequences

NOTES:

1. Input or trigger RNA sequences are listed up to the base immediately before the T7 terminator used to terminate transcription.

2. Gate RNA sequences are listed up to the 30th base (inclusive) following the end of their trigger binding domain. This 30-nt sequence contains the 21-nt linker sequence and the first 9-nts of GFPmut3b.

A. 2-input Toehold Repressor NAND Gate Circuit

Gate RNA	Gate Plasmid	Gate Plasmid Origin/Resistance	Input A1 Sequence	Input A2 Sequence	Non-Cognate RNA C Sequence	Non-Cognate RNA D Sequence	Triggers for Input 11	Triggers for Input 10	Triggers for Input 01	Triggers for Input 00	Trigger Plasmid Origin/Resistance
GGGAAGAAGAAAGAAGAUGGUAUUGGUAGAGGGUGUAAGAUACACAAUACAAACAA CUAUCAUUCACCUUCACAUACAAACAGAGGAGAUGGAGAUGGGAAAGAUAA ACCUGGCCAGCGCAAAGAUUCGCUAAA	pJK_NNAND1_RR07	ColA/kanamycin	GGGCUAUUGUGUAG UGUGUCACCAUAGG GACAUACUUCUACCC UCUUCACCAUACAG AUAAACGACGAUACA AUAGUAC	GGGUCAUGGCCAC UUCAUUGCUGGC UAGAAUUCUAGUUG UACUUCUCAUUA CGUCAUUCUCAU CAUCUAC	GGCCAAGAACGGGU UACCGGUUCUJGGAC UAAUUCACCAUUC UACACUAAACUAGC UUGCCGUCUCAUA UACAUU	GGGUCAUCAGCCCUC ACGUUGGGUGAGAU GAGCCUCGUCUCC AUGACGAGGCAACGU GGAUCGACUGAUCC UACAUU	A1, A2	A1, D	C, A2	C, D	ColE1/ampicillin, CDF/spectinomycin

B. 2-input 3WJ Repressor NAND Gate Circuits

Gate RNA	3WJ Repressor Switch Indices in Gate	Gate Plasmid	Gate Plasmid Origin/Resistance	3WJ Repressor Trigger Indices for Input 11	3WJ Repressor Trigger Indices for Input 10	3WJ Repressor Trigger Indices for Input 01	3WJ Repressor Trigger Indices for Input 00	Input Plasmid Origin/Resistance	Device ID
GGGACAAUCAAAUACAAUJGUUAJGLUULAGAACAGAGGAGA CAUACAUAGAACAAUACAUACAAAGCAACGACAAUACAAAA UACAUACAGAACAUUACUJGUUAJGUUAJGUAGAACAGAGGAC AUAAACAUAGAACACCUACAGACUACACUACGGCGC AGCGCAAAGAUUCGCUAAA	13, 19	pYZ_NAND2_L11_S13_S19	ColA/kanamycin	13, 19	13, 12	12, 19	12, 12	ColE1/ampicillin, CDF/Spectinomycin	N1
GGGACAAUCAAAUACAAUJGUUAJGUUAJGUAGAACAGAGGAGA CAUACAUAGAACAAUACAUACAAAGCAACGACAAUACACCG ACUCUCAUACAUACAUUJGUUAJGUUAJGUAGAACAGAGGAC AUAAACAUAGAACACCUACAGACUACACUACGGCGC AGCGCAAAGAUUCGCUAAA	13, 24	pYZ_NAND2_L11_S13_S24	ColA/kanamycin	13, 24	13, 12	12, 24	12, 12	ColE1/ampicillin, CDF/Spectinomycin	N2
GGGACAAUCAAAUACAAUJGUUAJGUUAJGUAGAACAGAGGAGA CAUACAUAGAACAAUACAUACAAUACUACAUACAUJGU AUACAUCAAAUACAUACAUUJGUUAJGUUAJGUAGAACAGAGGAC AUAAACAUAGAACACCUACAGACUACACUACGGCGC AGCGCAAAGAUUCGCUAAA	11, 13	pYZ_NAND2_L11_S11_S13	ColA/kanamycin	11, 13	11, 12	12, 13	12, 12	ColE1/ampicillin, CDF/Spectinomycin	N3
GGGACAAUCAAAUACAAUJGUUAJGUUAJGUAGAACAGAGGAGA CAUACAUAGAACAAUACAUACAAUACUACAUACAUJGU AUAAACAUACAUACAUUJGUUAJGUUAJGUAGAACAGAGGAC AUAAACAUAGAACACCUACAGACUACACUACGGCGC AGCGCAAAGAUUCGCUAAA	13, 10	pYZ_NAND2_L11_S13_S10	ColA/kanamycin	13, 10	13, 12	12, 10	12, 12	ColE1/ampicillin, CDF/Spectinomycin	N4
GGGACAAUCAAAUACAAUJGUUAJGUUAJGUAGAACAGAGGAGA CAUACAUAGAACAAUACAUACAAUACUACAUACAUJGU AUAAACAUACAUACAUUJGUUAJGUUAJGUAGAACAGAGGAC AUAAACAUAGAACACCUACAGACUACACUACGGCGC AGCGCAAAGAUUCGCUAAA	24, 13	pYZ_NAND2_L11_S24_S13	ColA/kanamycin	24, 13	24, 12	12, 13	12, 12	ColE1/ampicillin, CDF/Spectinomycin	N5
GGGACAAUCAAAUACAAUJGUUAJGUUAJGUAGAACAGAGGAGA CAUACAUAGAACAAUACAUACAAUACUACAUACAUJGU AUAAACAUACAUACAUUJGUUAJGUUAJGUAGAACAGAGGAC AUAAACAUAGAACACCUACAGACUACACUACGGCGC AGCGCAAAGAUUCGCUAAA	13, 21	pYZ_NAND2_L11_S13_S21	ColA/kanamycin	13, 21	13, 12	12, 21	12, 12	ColE1/ampicillin, CDF/Spectinomycin	N6
GGGACAAUCAAAUACAAUJGUUAJGUUAJGUAGAACAGAGGAGA CAUACAUAGAACAAUACAUACAAUACUACAUACAUJGU AUAAACAUACAUACAUUJGUUAJGUUAJGUAGAACAGAGGAC AUAAACAUAGAACACCUACAGACUACACUACGGCGC AGCGCAAAGAUUCGCUAAA	19, 13	pYZ_NAND2_L11_S19_S13	ColA/kanamycin	19, 13	19, 12	12, 13	12, 12	ColE1/ampicillin, CDF/Spectinomycin	N7
GGGACAAUCAAAUACAAUJGUUAJGUUAJGUAGAACAGAGGAGA CAUACAUAGAACAAUACAUACAAUACUACAUACAUJGU AUAAACAUACAUACAUUJGUUAJGUUAJGUAGAACAGAGGAC AUAAACAUAGAACACCUACAGACUACACUACGGCGC AGCGCAAAGAUUCGCUAAA	24, 19	pYZ_NAND2_L11_S24_S19	ColA/kanamycin	24, 19	24, 12	12, 19	12, 12	ColE1/ampicillin, CDF/Spectinomycin	N8
GGGACAAUCAAAUACAAUJGUUAJGUUAJGUAGAACAGAGGAGA CAUACAUAGAACAAUACAUACAAUACUACAUACAUJGU AUAAACAUACAUACAUUJGUUAJGUUAJGUAGAACAGAGGAC AUAAACAUAGAACACCUACAGACUACACUACGGCGC AGCGCAAAGAUUCGCUAAA	13, 19	pYZ_NAND2_L17_S13_S19	ColA/kanamycin	13, 19	13, 12	12, 19	12, 12	ColE1/ampicillin, CDF/Spectinomycin	N9
GGGACAAUCAAAUACAAUJGUUAJGUUAJGUAGAACAGAGGAGA CAUACAUAGAACAAUACAUACAAUACUACAUACAUJGU AUAAACAUACAUACAUUJGUUAJGUUAJGUAGAACAGAGGAC AUAAACAUAGAACACCUACAGACUACACUACGGCGC AGCGCAAAGAUUCGCUAAA	13, 10	pYZ_NAND2_L17_S13_S10	ColA/kanamycin	13, 10	13, 12	12, 10	12, 12	ColE1/ampicillin, CDF/Spectinomycin	N10
GGGACAAUCAAAUACAAUJGUUAJGUUAJGUAGAACAGAGGAGA CAUACAUAGAACAAUACAUACAAUACUACAUACAUJGU AUAAACAUACAUACAUUJGUUAJGUUAJGUAGAACAGAGGAC AUAAACAUAGAACACCUACAGACUACACUACGGCGC AGCGCAAAGAUUCGCUAAA	13, 11	pYZ_NAND2_L17_S13_S11	ColA/kanamycin	13, 11	13, 12	12, 11	12, 12	ColE1/ampicillin, CDF/Spectinomycin	N11
GGGACAAUCAAAUACAAUJGUUAJGUUAJGUAGAACAGAGGAGA CAUACAUAGAACAAUACAUACAAUACUACAUACAUJGU AUAAACAUACAUACAUUJGUUAJGUUAJGUAGAACAGAGGAG AUCAACAUACAUACAUACAUACAUACAUACAUACAUJGU GGAGACAUACAUACAUACAUACAUACAUACAUACAUACAU GGCGCGACGCCAAAAGAUUCGCUAAA	19, 13	pYZ_NAND2_L17_S19_S13	ColA/kanamycin	19, 13	19, 12	12, 13	12, 12	ColE1/ampicillin, CDF/Spectinomycin	N12
GGGACAAUCAAAUACAAUJGUUAJGUUAJGUAGAACAGAGGAGA CAUACAUAGAACAAUACAUACAAUACUACAUACAUJGU AUAAACAUACAUACAUUJGUUAJGUUAJGUAGAACAGAGGAG AUCAACAUACAUACAUACAUACAUACAUACAUACAUJGU GGAGACAUACAUACAUACAUACAUACAUACAUACAU GGCGCGACGCCAAAAGAUUCGCUAAA	24, 13	pYZ_NAND2_L17_S23_S13	ColA/kanamycin	24, 13	24, 12	12, 13	12, 12	ColE1/ampicillin, CDF/Spectinomycin	N13
GGGACAAUCAAAUACAAUJGUUAJGUUAJGUAGAACAGAGGAGA CAUACAUAGAACAAUACAUACAAUACUACAUACAUJGU AUAAACAUACAUACAUUJGUUAJGUUAJGUAGAACAGAGGAG AUCAACAUACAUACAUACAUACAUACAUACAUACAUJGU GGAGACAUACAUACAUACAUACAUACAUACAUACAU GGCGCGACGCCAAAAGAUUCGCUAAA	24, 19	pYZ_NAND2_L17_S24_S19	ColA/kanamycin	24, 19	24, 12	12, 19	12, 12	ColE1/ampicillin, CDF/Spectinomycin	N14

GGGAUCAUCAUUCUACUUCUUGGUUAUAGGUUAUGAACAGAGGAG ACAUACAGAACAAUACAUAAACCUAAGACUAAAGCGGACA AUACUACAUAAUAGAACAGACUUCUUGGUUAUAGUAJAGAACAG AGGAGACAUAAUAGAACAGACUACAAAGACAUAAUCAAC UGGGGGCAGCGCAAAGAUGCGUAAA	11, 19	pYZ_NAND2_L17_S11_S19	ColA/kanamycin	11, 19	11, 12	12, 19	12, 12	ColE1/ampicillin, CDF/Spectinomycin	N15
GGGACAUAAUAGAACUACUUCUUGGUUAUAGGUUAUGAACAGAGGAG ACAUACAGAACAAUACAUAAACCUAAGACUAAAGCGGACA ACCUCCAAUACAUAAUAGAACAGACUUCUUGGUUAUAGUAJAGAACAG AGGAGACAUAAUAGAACAAUACAUAAACCUAAGACAUAAACC UGGGGGCAGCGCAAAGAUGCGUAAA	19, 11	pYZ_NAND2_L17_S19_S11	ColA/kanamycin	19, 11	19, 12	12, 11	12, 12	ColE1/ampicillin, CDF/Spectinomycin	N16 (used in Figure 5 of main text)

C. 2-Input 3WJ Repressor NOR Gate Circuit

Gate RNA	3WJ Repressor Switch Index in Gate	Gate Plasmid	Gate Plasmid Origin/Resistance	Trigger A Sequence	Trigger B Sequence	Non-Cognate RNA C Sequence	Non-Cognate RNA D Sequence	Triggers for Input 11	Triggers for Input 10	Triggers for Input 01	Triggers for Input 00	Trigger Plasmid Origin/Resistance
GGGAGUUAAGAUUAAGCGCUUAGGUUAUGGUUAUGAACAGAGGAC UAUAGUUGUAGUGUCGGAUAGGUAGGUAGUAGUAGUACAUCA CAUCAAGGCCAUAAUUCGGAAGACUAGGUAGGUAGGUAG GUAGUAGUAGUAGGUAGGACACUACAUAGGUAGGUAGCGGAU AAGUAGUAGUAGGUACAUUCAUCAUACACUCAUAC GAGGACAGACUACAUUCAUACAUAGGUAGGUAGGUAG AGGAGACAUAAUAGAACAAUCCGACACUACAUAAUUCGGAACC UGGGGGCAGCGCAAAGAUGCGUAAA	21	pYZ_NOR2_HpEF	ColA/kanamycin	GGGUGACAUUACUCAA GAGCGGAUAGUAGUAC UAACAUCAACAUAA CGCUUCUAAUCUUA CU	GGGAGCUGGGCAG CUUCUACUGGCCA CGUCAUCUCAA UCUAAUCAUAA UAGGUAGUAG	GGGACGAUUAUACGGGU CUACGUUAUACGUACA AGAACCAUACAGACAA CGACGACACUAGA	A, B	A, C	B, C	C, D	ColE1/ampicillin, CDF/spectinomycin	

D. 3-Input 3WJ Repressor NAND Gate Circuits

Gate RNA	3WJ Repressor Switch Indices in Gate	Gate Plasmid	Gate Plasmid Origin/Resistance	3WJ Repressor Trigger Indices for Input 111	3WJ Repressor Trigger Indices for Input 011	3WJ Repressor Trigger Indices for Input 101	3WJ Repressor Trigger Indices for Input 110	3WJ Repressor Trigger Indices for Input 100	3WJ Repressor Trigger Indices for Input 010	3WJ Repressor Trigger Indices for Input 001	3WJ Repressor Trigger Indices for Input 000	Input Plasmid Origin/Resistance	Device ID
GGGCUCCUAACUUUACUUCUUGGUUAUAGGUUAUGAACAGAGGAG ACAUACAGAACACAGCACUACAUAAACCUAAGAACAGCCAC AUACAUACAGAACAUCAUCUUGGUUAUAGGUAGAACAGAGGAG CAUACUAGAACACUACAUACAUAAUUCGGAACAUACAU CACAAUCAACAAUCAUUQUAUQUAUAGGUAGAACAGAGGAG UAACAGAACAAUCAACAUACAAAGAACGAAACGAAAC CGCGAAAAGAUICGGUAAA	24, 19, 13	pYZ_NAND3_L11_S24_S19_S13	ColA/kanamycin	(19, 24), 13	12, (19, 24)	13, (12, 24)	13, (24, 12)	12, (13, 12)	(12, 12), 19	(12, 12), 24	(12, 12), 12	ColE1/ampicillin, CDF/Spectinomycin	N1
GGGACAUAAUAGAACUACUUCUUGGUUAUAGGUUAUGAACAGAGGAG ACAUACAGAACACAGCACUACAUAAACCUAAGAACACAU AUACAUAGAACAUACAUACAUAAUUCGGAACAUACAU CACAAUCAACAAUCAUUQUAUQUAUAGGUAGAACAGAGGAG UAACAGAACAAUCAACAUACAAAGAACGAAACGAGAAC CGCGAAAAGAUICGGUAAA	19, 24, 13	pYZ_NAND3_L11_S19_S24_S13	ColA/kanamycin	(19, 24), 13	12, (19, 24)	13, (24, 12)	13, (19, 12)	12, (13, 12)	(12, 12), 19	(12, 12), 24	(12, 12), 12	ColE1/ampicillin, CDF/Spectinomycin	N2
GGGAUCAUCAUACAUUACUUCUUGGUUAUAGGUUAUGAACAGAGGAG ACAUACAGAACACAGCACUACAUAAACCUAAGAACACAU AUACAUAGAACAUACAUACAUAAUUCGGAACAUACAU CACAUACAGAACAUACAUACAUAAUUCGGAACAUACAU AACAUACAGAACAUACAUACAUAAUUCGGAACAUACAU CGCGAAAAGAUICGGUAAA	11, 13, 19	pYZ_NAND3_L11_S11_S13_S19	ColA/kanamycin	(11, 19), 13	13, (12, 19)	11, (19, 12)	11, (13, 12)	(11, 12), 12	(12, 12), 19	(12, 12), 13	(12, 12), 12	ColE1/ampicillin, CDF/Spectinomycin	N3 (used in Figure 6 of main text)
GGGUCUCUUAUACUUCUUGGUUAUAGGUUAUGAACAGAGGAG ACAUACAGAACACAGCACUACAUAAACCUAAGAACACAU AUACAUAGAACAUACAUACAUAAUUCGGAACAUACAU AUACAUAGAACAUACAUACAUAAUUCGGAACAUACAU AACAUACAGAACAUACAUACAUAAUUCGGAACAUACAU CGCGAAAAGAUICGGUAAA	24, 13, 19	pYZ_NAND3_L11_S24_S13_S19	ColA/kanamycin	(19, 24), 13	12, (19, 24)	13, (24, 12)	13, (19, 12)	12, (13, 12)	(12, 12), 19	(12, 12), 24	(12, 12), 12	ColE1/ampicillin, CDF/Spectinomycin	N4
GGGACAUAAUACAAUAAUUGGUUAUAGGUUAUGAACAGAGGAG CAUACAUAGAACAUACAUAAACCUAAGAACACAU AUACAUAGAACAUACAUACAUAAUUCGGAACAUACAU AUACAUAGAACAUACAUACAUAAUUCGGAACAUACAU AACAUACAGAACAUACAUACAUAAUUCGGAACAUACAU AACCUUGGGCAGCGCAAAGAUICGGUAAA	13, 11, 19	pYZ_NAND3_L17_S13_S11_S19	ColA/kanamycin	(11, 19), 13	13, (12, 19)	11, (19, 12)	11, (13, 12)	(11, 12), 12	(13, 12), 12	(12, 12), 19	(12, 12), 12	ColE1/ampicillin, CDF/Spectinomycin	N5
GGGACAUAAUACAUUACUUCUUGGUUAUAGGUUAUGAACAGAGGAG CAUACAUAGAACAUACAUAAACCUAAGAACACAU GGAGACAUAAUACAUACAUAAUUCGGAACAUACAU CGCGAAAAGAUICGGUAAA	19, 13, 11	pYZ_NAND3_L17_S19_S13_S11	ColA/kanamycin	(11, 19), 13	13, (12, 19)	11, (19, 12)	11, (13, 12)	(11, 12), 12	(13, 12), 12	(12, 12), 19	(12, 12), 12	ColE1/ampicillin, CDF/Spectinomycin	N6

E. NOT ((A1 AND A2) OR (B1 AND B2)) Circuit

Supplementary Table 11. Descriptions of Thermodynamic Parameters Used for Automated Forward Engineering

Group	Parameter Name	Parameter Description
MFE of RNA strands and critical RNA subsequences	deltaG_hpin	The minimum free energy (MFE) of the switch (or hairpin) RNA running from the 5' end to 29th base of the GFP coding sequence.
	deltaG_targ	The MFE of the trigger (or target) RNA from the 5' end to the end of the terminator sequence.
	deltaG_comp	The MFE of the complex formed between the switch RNA sequence defined above and the full trigger RNA.
	deltaG_min_hpin	The MFE of the minimal switch RNA sequence from the 5' end to the base immediately before the start of the 21-nt linker sequence.
	deltaG_min_targ	The MFE of the 45-nt minimal trigger RNA sequence that is programmed to bind to the switch RNA.
	deltaG_min_comp	The MFE of the complex formed between the minimal switch RNA sequence and the minimal trigger RNA sequence.
	deltaG_min_stem_recon	The MFE of the hairpin secondary structure that forms to repress translation once the trigger RNA binds; this sequence comprises the 18-nt repressing stem along with the RBS and start codon.
Measures of binding for critical RNA domains	deltaG_toeh_binding	The free energy of the 15-nt toehold sequence of the repressor when base pairing perfectly to its reverse complement.
	deltaG_targ_binding	The free energy of the 45-nt minimal trigger RNA sequence when base pairing perfectly to its reverse complement sequence
	deltaG_toeh_binding_actual	The MFE of the 15-nt toehold sequence of the repressor bound to its reverse complement sequence; this MFE structure may have unpaired bases at the ends of the duplex.
	deltaG_targ_binding_actual	The MFE of the 45-nt minimal trigger RNA sequence bound to its reverse complement sequence; this MFE structure may have unpaired bases at the ends of the duplex.
Net reaction free energies	net_deltaG_comp	The net free energy change upon formation of the trigger/switch RNA complex; it is equal to deltaG_comp - deltaG_hpin - deltaG_targ.
	net_deltaG_min_comp	The net free energy change upon formation of the trigger/switch RNA complex based on the minimal trigger and switch sequences; it is equal to deltaG_min_comp - deltaG_min_hpin - deltaG_min_targ.
Influence of coding sequence secondary structure on translation in active state	dup2mRNA_deltaG	The MFE of the RNA sequence starting from the first base after the switch RNA stem (nucleotide 88) through to the 29th base of the GFP coding sequence
	dup2link_deltaG	The MFE of the RNA sequence starting from the first base after the switch RNA stem (nucleotide 88) through to the end of the 21-nt linker sequence (nucleotide 138, just before the beginning of the GFP sequence).
	dup2pos03_deltaG	The MFE of the RNA sequence starting from the first base after the switch RNA stem (nucleotide 88) through to the Nth base of the GFP coding sequence, where N = 3, 6, 9, etc.
	dup2pos06_deltaG	
	dup2pos09_deltaG	
	dup2pos12_deltaG	
	dup2pos15_deltaG	
	dup2pos18_deltaG	
	dup2pos21_deltaG	
	dup2pos24_deltaG	
	dup2pos27_deltaG	
	AUG2mRNA_deltaG	The MFE of the RNA sequence starting from the start codon of the switch RNA (nucleotide 106) through to the 29th base of the GFP coding sequence.
	dup2AUG_deltaG	The MFE of the RNA sequence starting from the first base after the switch RNA stem (nucleotide 88) through to the end of the switch RNA start codon (nucleotide 108).
Influence of coding sequence secondary structure on translation in inactive state	recon_dup2mRNA_deltaG	The MFE of the RNA sequence starting from the first base after the trigger RNA binding site on the switch RNA (nucleotide 49) through to the 29th base of the GFP coding sequence.
	recon_dup2link_deltaG	The MFE of the RNA sequence starting from the first base after the trigger RNA binding site on the switch RNA (nucleotide 49) through to the end of the 21-nt linker sequence (nucleotide 138, just before the beginning of the GFP sequence).
	recon_dup2pos03_deltaG	The MFE of the RNA sequence starting from the first base after the trigger RNA binding site on the switch RNA (nucleotide 49) through to the Nth base of the GFP coding sequence, where N = 3, 6, 9, etc.
	recon_dup2pos06_deltaG	
	recon_dup2pos09_deltaG	
	recon_dup2pos12_deltaG	
	recon_dup2pos15_deltaG	
	recon_dup2pos18_deltaG	
	recon_dup2pos21_deltaG	
	recon_dup2pos24_deltaG	
	recon_dup2pos27_deltaG	
Deviations of actual sequence from the ideal, design-specified secondary structure	dev_deltaG_hpin	The difference in energy obtained by subtracting deltaG_hpin from the free energy of the switch RNA sequence when it is folded in the ideal, design-specified secondary structure.
	dev_deltaG_targ	The difference in energy obtained by subtracting deltaG_targ from the free energy of the trigger RNA sequence when it is folded in the ideal, design-specified secondary structure.
	dev_deltaG_comp	The difference in energy obtained by subtracting deltaG_comp from the free energy of the trigger/switch RNA complex when it is folded in the ideal, design-specified secondary structure.
	dev_deltaG_min_hpin	The difference in energy obtained by subtracting deltaG_min_hpin from the free energy of the minimal switch RNA sequence when it is folded in the ideal, design-specified secondary structure.

dev_deltaG_min_targ	The difference in energy obtained by subtracting deltaG_min_targ from the free energy of the minimal trigger RNA sequence when it is folded in the ideal, design-specified secondary structure.
dev_deltaG_min_comp	The difference in energy obtained by subtracting deltaG_min_comp from the free energy of the trigger/switch RNA complex generated from the minimal sequences when it is folded in the ideal, design-specified secondary structure.
dev_recon_dup2mRNA_deltaG	The difference in energy obtained by subtracting recon_dup2mRNA_deltaG from the free energy of that sequence (i.e. the one used for calculating recon_dup2mRNA_deltaG) in the ideal, design-specified secondary structure, which contains a translation-repressing hairpin structure.
dev_recon_dup2link_deltaG	The difference in energy obtained by subtracting recon_dup2link_deltaG from the free energy of that sequence in the ideal, design-specified secondary structure.
dev_recon_dup2pos03_deltaG	The difference in energy obtained by subtracting recon_dup2posN_deltaG from the free energy of that sequence in the ideal, design-specified secondary structure, where N = 3, 6, 9, etc.
dev_recon_dup2pos06_deltaG	
dev_recon_dup2pos09_deltaG	
dev_recon_dup2pos12_deltaG	
dev_recon_dup2pos15_deltaG	
dev_recon_dup2pos18_deltaG	
dev_recon_dup2pos21_deltaG	
dev_recon_dup2pos24_deltaG	
dev_recon_dup2pos27_deltaG	
Measures of switch RNA stem sequence and secondary structure	deltaG_stem_01 This set of parameters was calculated starting from the 69-nt sequence of the main switch RNA hairpin, which consisted of a 30-nt stem and a 9-nt loop. The main switch RNA hairpin was then analyzed for different subsequences corresponding to different stem lengths. deltaG_stem_01 is the MFE of nucleotides 1 to 69, deltaG_stem_02 is the MFE of nucleotides 2 to 68, etc.
	deltaG_stem_02
	deltaG_stem_03
	deltaG_stem_04
	deltaG_stem_05
	deltaG_stem_06
	deltaG_stem_07
	deltaG_stem_08
	deltaG_stem_09
	deltaG_stem_10
	deltaG_stem_11
	deltaG_stem_12
	deltaG_stem_13
	deltaG_stem_14
	deltaG_stem_15
	deltaG_stem_16
	deltaG_stem_17
	deltaG_stem_18
	deltaG_stem_19
	deltaG_stem_20
	deltaG_stem_21
	deltaG_stem_22
	deltaG_stem_23
	deltaG_stem_24
	deltaG_stem_25
	deltaG_stem_26
	deltaG_stem_27
	deltaG_stem_28
	deltaG_stem_29
	deltaG_stem_30
min_bot_deltaG_01 min_bot_deltaG_02 min_bot_deltaG_03 min_bot_deltaG_04 min_bot_deltaG_05 min_bot_deltaG_06 min_bot_deltaG_07 min_bot_deltaG_08 min_bot_deltaG_09 min_bot_deltaG_10 min_bot_deltaG_11 min_bot_deltaG_12 min_bot_deltaG_13 min_bot_deltaG_14 min_bot_deltaG_15 min_bot_deltaG_16 min_bot_deltaG_17 min_bot_deltaG_18 min_bot_deltaG_19 min_bot_deltaG_20 min_bot_deltaG_21 min_bot_deltaG_22 min_bot_deltaG_23	This set of parameters was calculated using the 5' and 3' arms of the main switch RNA hairpin. The 5' and 3' arms comprised nucleotides 19 to 48 and 58 to 87 of the switch RNA sequence, respectively. For the purposes of the calculation, subsequences from the 5' and 3' arms were joined using the sequence AAAAAAAA and their MFE computed. min_bot_deltaG_02, for instance, has the 1st through 29th bases of the 5' arm, the poly-A loop, and the 2nd through 30th bases of the 3' arm.

min_bot_deltaG_24
min_bot_deltaG_25
min_bot_deltaG_26
min_bot_deltaG_27
min_bot_deltaG_28
min_bot_deltaG_29
min_bot_deltaG_30

Supplementary Note. Toehold Repressor Forward Engineering

A second-generation toehold repressor library was generated through an automated forward engineering procedure based on sequence-dependent thermodynamic parameters and GFP output obtained from the initial library of toehold repressors. A set of 114 easy-to-calculate thermodynamic parameters was defined as shown in Supplementary Table 11. The parameters were calculated using the subsequences, or sequence windows, also specified in Supplementary Table 11. These parameters can be broadly classified into seven different categories.

1. *MFE of RNA strands and critical RNA subsequences:* The minimum free energy (MFE) of the RNA strands and subsequences was calculated to assess the strength of the repressor secondary structures and the binding between trigger and switch RNAs.
2. *Measures of binding for critical RNA domains:* The free energies of duplex structures formed between toehold domains and 45-nt minimal trigger sequences were calculated to assess the binding strengths of these interactions. The duplexes were simulated as two separate molecules that hybridize with one another.
3. *Net reaction free energies:* The net change in free energy starting from separate trigger and switch RNA strands and ending with the trigger-switch complex.
4. *Influence of coding sequence secondary structure on translation in active state:* The MFEs for the coding sequence over different subsequences of the switch RNA were used to assess the efficiency with which these regions would be translated.
5. *Influence of coding sequence secondary structure on translation in inactive state:* The MFE for the switch RNA subsequence immediately after the binding site for the trigger RNA was used to assess the degree of translation inhibition caused by sequestering the RBS and start codon in a stem loop. These parameters were also calculated over several switch RNA subsequences.
6. *Deviations of actual sequence from the ideal, design-specified secondary structure:* These parameters were used to assess the degree to which the predicted MFE structures differed from those specified in the toehold switch design. We expected that these parameters would capture, for instance, designs where base pairing within the toehold domain reduced the performance of the repressor.
7. *Measures of switch RNA stem sequence:* These parameters evaluated the strength of the switch RNA stem over different sequence ranges starting from the top or the bottom of the stem. Previous studies with toehold switches had revealed some performance improvements when a stem had A-U base pairs at particular locations. We expected that these parameters could capture such effects in the toehold repressors.

The thermodynamic parameters were calculated for 38 toehold repressors from the first-generation library using a local implementation of the NUPACK 3.0 functions `mfe`, `energy`, and `complexes` with Mathews et al., 1999 energy parameters¹. Six devices were excluded from the analysis due to their unusually low ON state expression level or high expression variability in either the ON or OFF state. A series of different linear regressions were then performed using the thermodynamic parameters and $\log_{10}(\text{GFP fold reduction})$ obtained from the repressor library. These regressions were calculated using the Matlab `regress` function, which implemented a multiple linear regression algorithm using least squares. Supplementary Figure 9 provides a map of R^2 values obtained for all two-parameter linear regressions performed using the 114 thermodynamic parameters. This analysis identified several parameters showing stronger correlations with the experimental data and suggested extension of the approach to three-parameter regressions.

To develop a scoring function to rank potential toehold repressors, all possible combinations of up to three different thermodynamic parameters were first computed (Supplementary Figure 10a). This search was limited to three parameters to evaluate a number of parameter combinations that could be computed reasonably quickly, since the number of combinations increases exponentially with the number of fitting parameters. The resulting 253,460 linear regressions were then ranked from highest to lowest R^2 value. Supplementary Figure 10b displays the best three-parameter linear regression obtained from experimental measurements of GFP fold reduction, which provided a coefficient of determination R^2 of 0.422. Regression coefficients from the top 10 linear regressions were extracted to generate an overall scoring function. The combined regression coefficients were generated using equation (1):

$$B_i = \frac{1}{N} \sum_{j=1}^N C_{ij} \quad (1)$$

where B_i is the combined regression coefficient for parameter i , C_{ij} is the regression coefficient for parameter i in regression j , and $N = 10$ is the number of regressions combined. In cases where parameter i was not used in the linear regression, the regression coefficient was equal to zero. The scoring function for ranking designs was then of the following form:

$$S_k = \sum_i B_i \Delta G_{ik} \quad (2)$$

where S_k is the score computed for toehold repressor design k and ΔG_{ik} is the free energy calculated for parameter i for toehold repressor design k . Repressors predicted to offer higher performance were thus given higher scores. The final equation for the scoring function, using the parameter names from Supplementary Table 11, is:

$$\begin{aligned} S_k = & 0.025 \times \text{deltaG_toeh_binding}_k + 0.025 \times \text{deltaG_toeh_binding_actual}_k \\ & + 0.003 \times \text{deltaG_targ_binding}_k + 0.003 \times \text{deltaG_targ_binding_actual}_k \\ & + 0.377 \times \text{deltaG_stem_27}_k + 0.029 \times \text{dup2link_deltaG}_k \\ & + 0.029 \times \text{dup2pos03_deltaG}_k - 0.072 \times \text{deltaG_stem_26}_k \\ & - 0.021 \times \text{deltaG_stem_25}_k \end{aligned} \quad (3)$$

This automatically generated scoring function was then applied to a set of 265 new toehold repressor sequences produced using the same sequence and structural parameters as the first-generation library. For these designs, the values of several thermodynamic parameters were identical or nearly identical to one another across the set of sequences, enabling the scoring function to be simplified to the following expression:

$$\begin{aligned} S_k = & 0.050 \times \text{deltaG_toeh_binding}_k + 0.006 \times \text{deltaG_targ_binding}_k \\ & + 0.058 \times \text{dup2link_deltaG}_k + 0.377 \times \text{deltaG_stem_27}_k \\ & - 0.072 \times \text{deltaG_stem_26}_k - 0.021 \times \text{deltaG_stem_25}_k \end{aligned} \quad (4)$$

The 96 new repressor sequences providing the highest scores were then assembled and tested. These devices yielded substantially improved performance compared to the first-generation library, with over 84% of the riboregulators providing at least 10-fold reductions in GFP expression compared to 48% for the initial library (Figure 2). The improvements were more striking on the high end of device performance with only one device (2%) in the first-generation library with 100-fold reduction in GFP compared to 8 devices (8%) in the second-generation set. Since this forward-engineering approach can lead to better device performance, it is likely that more computationally intensive studies with more than three parameters can be used to obtain improved riboregulator libraries.

Analysis of the thermodynamic parameters and regression coefficients used in the scoring function provides some insight into the riboregulator characteristics favored for the

second-generation library. The terms deltaG_toeh_binding and deltaG_targ_binding provided the largest overall contributions to the device score and encouraged selection of sequences with weaker binding through the toehold and minimal trigger regions. In effect, these parameters favored devices with low GC content in the toehold and trigger region. The next most important term was dup2link_deltaG, which also had a positive regression coefficient. This term measures the secondary structure of the switch RNA region being translated when the riboregulator is in its ON state. Accordingly, this term favored devices with low secondary structure in this region to encourage efficient translation of the output protein. The last three terms in the scoring function are related to the free energy of subsequences near the top of the switch RNA stem. The deltaG_stem_27 has a positive regression coefficient and thus selected for designs having low GC content in the top four base pairs at the top of the switch stem. In contrast, deltaG_stem_26 and deltaG_stem_25, which assessed five and six base-pair upper stems, respectively, had negative coefficients and thus favored stronger base pairing in the upper stem. Taken together, the last three parameters assigned higher scores to devices having low GC content in the top four base pairs of the stem and relatively higher GC content in the base pairs 5 and 6 nts from the stem top.

Supplementary Note References

1. D. H. Mathews, J. Sabina, M. Zuker & D. H. Turner, "Expanded sequence dependence of thermodynamic parameters improves prediction of RNA secondary structure," *Journal of Molecular Biology* **288**, 911-940 (1999).